UNIVERSITÀ DEGLI STUDI DI TRIESTE

SEDE AMMINISTRATIVA DEL DOTTORATO DI RICERCA

XXIV CICLO DEL
SCUOLA DI DOTTORATO IN
INGEGNERIA CIVILE E AMBIENTALE

IMPLEMENTATION OF LIDAR DATA IN HYDROLOGICAL MODEL TOPMODEL FOR PREDICTING FLOOD MONTICANO RIVER CASE STUDY

(Settore scientifico-disciplinare ICAR/05)

DOTTORANDO
NAHID KHODAYARI

COORDINATORE DEL COLLEGIO DEI DOCENTI
CHIAR.MO PROF. IGINIO MARSON
UNIVERSITÀ DEGLI STUDI DI TRIESTE

TUTORE
PROF. IGINIO MARSON
UNIVERSITÀ DEGLI STUDI DI TRIESTE

RELATORE
PROF. ELPIDIO CARONI
UNIVERSITÀ DEGLI STUDI DI TRIESTE

RELATORE
Dr. SADEGH YARI
ISTITUTO NAZIONALE DI OCEANOGRAFIA E DI GEOFISICA SPERIMENTALE - OGS

RELATORE
Dr. FRANCO COREN
ISTITUTO NAZIONALE DI OCEANOGRAFIA E DI GEOFISICA SPERIMENTALE - OGS

ANNO ACCADEMICO 2010/2011

UNIVERSITÀ DEGLI STUDI DI TRIESTE
SEDE AMMINISTRATIVA DEL DOTTORATO DI RICERCA

XXIV CICLO DEL

SCUOLA DI DOTTORATO IN
INGEGNERIA CIVILE E AMBIENTALE

IMPLEMENTATION OF LIDAR DATA IN HYDROLOGICAL MODEL TOPMODEL FOR PREDICTING FLOOD MONTICANO RIVER CASE STUDY

(Settore scientifico-disciplinare ICAR/05)

DOTTORANDO
NAHID KHODAYARI

COORDINATORE DEL COLLEGIO DEI DOCENTI
CHIAR.MO PROF. IGINIO MARSON
UNIVERSITÀ DEGLI STUDI DI TRIESTE

TUTORE
PROF. IGINIO MARSON
UNIVERSITÀ DEGLI STUDI DI TRIESTE

RELATORE
PROF. ELPIDIO CARONI
UNIVERSITÀ DEGLI STUDI DI TRIESTE

RELATORE
Dr. SADEGH YARI
ISTITUTO NAZIONALE DI OCEANOGRAFIA E DI GEOFISICA SPERIMENTALE - OGS

RELATORE
Dr. FRANCO COREN
ISTITUTO NAZIONALE DI OCEANOGRAFIA E DI GEOFISICA SPERIMENTALE - OGS

ANNO ACCADEMICO 2010/2011

To:

My wonderful family

Particularly to my understanding and patient husband, Sadegh

and to our precious daughter Rasta, who is the joy of our lives

WATER

Let's not muddy the stream.

Down the stream a pigeon seems to be drinking

Or perhaps in some farther thicket, a goldfinch is washing its plumage.

Or perhaps in some hamlet a jar is being filled.

Let's not muddy the stream.

This stream is perhaps running to the foot of a poplar tree to wash away the sorrows of some lonely heart.

A dervish is perhaps dipping a piece of dry bread into the stream.

A lovely lady has come to the lip of the stream.

Let's not muddy the stream.

Beauty is doubled.

What delicious water!

How clear a stream!

How cordial are the people in the upper hamlet!

May their streams jet out! May their cows give prodigious milk!

Never have I visited their hamlet.

There must be God's footprints at the foot of their hedges.

There, moonshine must be brightening over the expanse of speech.

Fences must be low in the upper hamlet.

Its inhabitants surely know what a flower the peony is.

There, blue must be blue

Some bud is blossoming; the hamlet inhabitants are aware of it.

What a glorious hamlet it must be!

May its alleyways overflow with music!

The people at the mouth of the stream appreciate water.

They have not muddied the stream.

Nor should we.

Poem by Sohrab Sepehri (October 7, 1928 - April 21, 1980)

Translated By A.Zahedi, I. Salami

TABLE OF CONTENTS

List of Figures

List of Tables

Acknowledgements

I would never have been able to finish my dissertation without the help and support of many people. Therefore, I would like to give my warm thanks to them.

First of all, I am grateful to my supervisor, Professor Iginio Marson for his constant support.

I would like to thank Professor Elpidio Caroni for his worthy helps during our collaboration and excellent hints and specially reviewing the manuscript.

Special thanks to Dr. Franco Coren (OGS) for his valuable help and providing the LiDAR data.

I owe my deepest gratitude to my husband who was also my advisor, Dr. Sadegh Yari (OGS) who guided me through this work and we had very beneficial discussions to develop the ideas and do the best. Without his help, this work would not be possible.

My sincere thanks go to Professor Rinaldo Nicolich, who encouraged me to participate in this PhD school.

I would also acknowledge Prof. K. Beven, Lancaster University, for his advices.

Many thanks go in particular to Dr. Dean Djokic, Water Resources Consulting and Custom Solutions Practice at Esri for his useful comments on GIS applications.

I warmly thank to ICTP library, which gave me opportunity to use needed sources for this work.

I am very grateful to ARPAV (Agenzia Regionale per la Prevenzione e protezione Ambientale del Veneto) to collaboration with me to provide hydrological data.

Thanks to Esri Italy for providing one-year student license for ArcGIS 10.

Where would I be without my family? My heartfelt appreciation also goes to my parents for their love, support and encouragement throughout my entire life, my father who taught me to be honest and my mother for giving birth to me! Now I know how pain she suffered for labor.

It is a pleasure to express my gratitude wholeheartedly to my lovely sisters Nazi and Samaneh for their loving supports.

My loving thanks are due to my brother in law Mehrdad Hedayat, who has tried to refresh my mind during this work by playing his violin.

Words fail me to express my appreciation to my adorable husband Sadegh whose dedication, love and persistent confidence in me, has taken the load off my shoulder. I owe him for being unselfishly let his intelligence, passions, and ambitions collide with mine.

There are no words to describe the emotional and loving way he supported me, undoubtedly, the biggest thanks are for him!

Last but not the least and most importantly, I would like to give heartfelt gratitude to our little (3 months old) lovely daughter Rasta for her patience during the last months of writing the dissertation.

Finally, I would like to thank everybody who was important to the successful realization of thesis, as well as expressing my apology that I could not mention personally one by one.

Abstract

The semi-distributed rainfall-runoff model, TOPOMODEL is applied to predict the response of Monticano River basin to rain events. TOPMODEL is a topographic based model in which the topographic index has an essential role. Topographic index is a function of the Digital Elevation Model (DEM) resolution.

The high resolution LiDAR data with 1-2 points per meter square, is used as topographic data to generate DEMs, calculate the topographic index as well as extracting the hydrological features. Due to significant effect of the DEM resolution on the topographic index and hydrological features accuracy, different DEMs with 25 m, 50 m, 100 m and 200 m grid size are generated using LiDAR data. Comparing the density function of topographic index with different resolutions indicate that by decreasing the resolution there is a shift toward the higher values as well as increasing the topographic constant λ from 7.36 for 25 m resolution to 10.32 corresponding to 200 m grid size.

TOPMODEL is applied to simulate the six events namely; 20-21 December 1997, 6-7 November 2000, 10-12 August 2002, 21-23 January 2003 , 31 October-1November 2004 and 22-26 December 2009. The model successfully simulates flood levels, with respect to both their extent and to peak time.

The sensitivity analysis for scale parameter m and lateral transmissivity T_0 shows that the coefficient m affects much more than T_0 on the hydrograph shape and peak value.

The effect of DEM resolution on the model results is examined. The model results are different, but the differences are very small except for events 2003 and 2009. The results of simulations based on 25 m grid size are very close to those of 50 m grid size, while the simulated discharges using 100 m and 200 m grid size are overestimated.

The efficiency of the simulations are calculated for all events using different topographic index distributions. The efficiency of model is in a range of 0.86 for event 2009 to 0.99 for event 2002. The high values of efficiency can be due to effect of accurate topographic index distribution and hydrological features extracted from high resolution topographic data.

The simulation based on DEM with 25 m resolution shows slightly higher efficiency values. This means that generating higher resolution DEM with respect to suggested 50 m grid size for TOPMODEL, may give a more accurate output as it is evident from this study.

Chapter One

Overview

1.1. Introduction

Today forecasting plays an important role in our life. It seems that the most important one is forecasting the climatic (in general) condition both in short time and long term due to its effect on our living system. The prediction of the long-term climatic condition, which is affected by climate change phenomena, is crucial for sustainable management and decision making in long time, and spatially, from small scale to even continental scale. On the other side, the short-term prediction is essential for daily life and even for avoiding damages due to rapid changes in the system.

The results of the meteorological observations and climate models (general circulation models and regional circulation models) usually are used as input for the hydrological models, which is mainly precipitation. The importance of hydrological modeling in prediction of flood and related hazard is more sensible in daily life.

On the other side, the new technologies for the observation, storing data, analyzing and forecasting enables us to study these phenomenon in the most possible details. Evolution of measuring systems, computational facilities and softwares, influenced the hydrological modeling in the way toward reliable predictions.

To have a complete understanding of our environment hydrology system we need to measure large number parameters for long time and in a wide area, which is impossible.

Practically we have a limit range of measurements (in time and space) and still limitations in measuring techniques. This leads us toward modeling, which is simply extrapolation from our limited data in time and space to predict the catchment response to hydrological changes in future and a better decision making.

1.2. Hydrological models

A hydrological model is a simplified system of governing laws of a watershed for evaluating the processes of the hydrological cycle in the entire basin or a part of it. It is based on a set of interrelated equations that try to convert the physical laws, which govern extremely complex natural phenomena, to abstract mathematical forms (Lastoria 2008).

Rainfall-runoff model is a hydrological model that predicts the runoff (or flood) in the watershed basin using the precipitation data. The precipitation data can be direct measurements, model results or combination of two methods. However, it should be noted that the topographic information has an undeniable role in the hydrological modeling.

According to Singh (1995) the rainfall-runoff models can be classified according to their degree of representation of the physical processes and to the spatial and temporal description (Melone et al., 2005).

Considering the physical processes of the model, rainfall-runoff models can be categorized as:

- Physically-based (white box) model
- Empirical or stochastic (black box) model
- Conceptual (grey box) model

All these three types of mathematical models represent different levels of approximation of reality. Physically-based models are the closest representation of the real system and try to incorporate as many components of actual physical processes as possible. Empirical models do not aid in physical understanding so that their parameters may have some little physical significance and can be estimated only by using concurrent measurements of input and output variables. Conceptual models may be considered intermediate between the two previous types of models, because they consider physical laws but in highly simplified form (Lastoria, 2008).

On the basis of the spatial representation, the hydrological models can be classified into three main categories:

- distributed models
- semi-distributed models
- lumped models

A distributed model represents spatial heterogeneity with a user defined resolution. These models can provide the highest accuracy in the modelling of rainfall-runoff processes (Cunderlik, 2003). The parameters of these models should be corresponding to each cell of the domain, therefore require considerably more input data (Fig. 1.1).

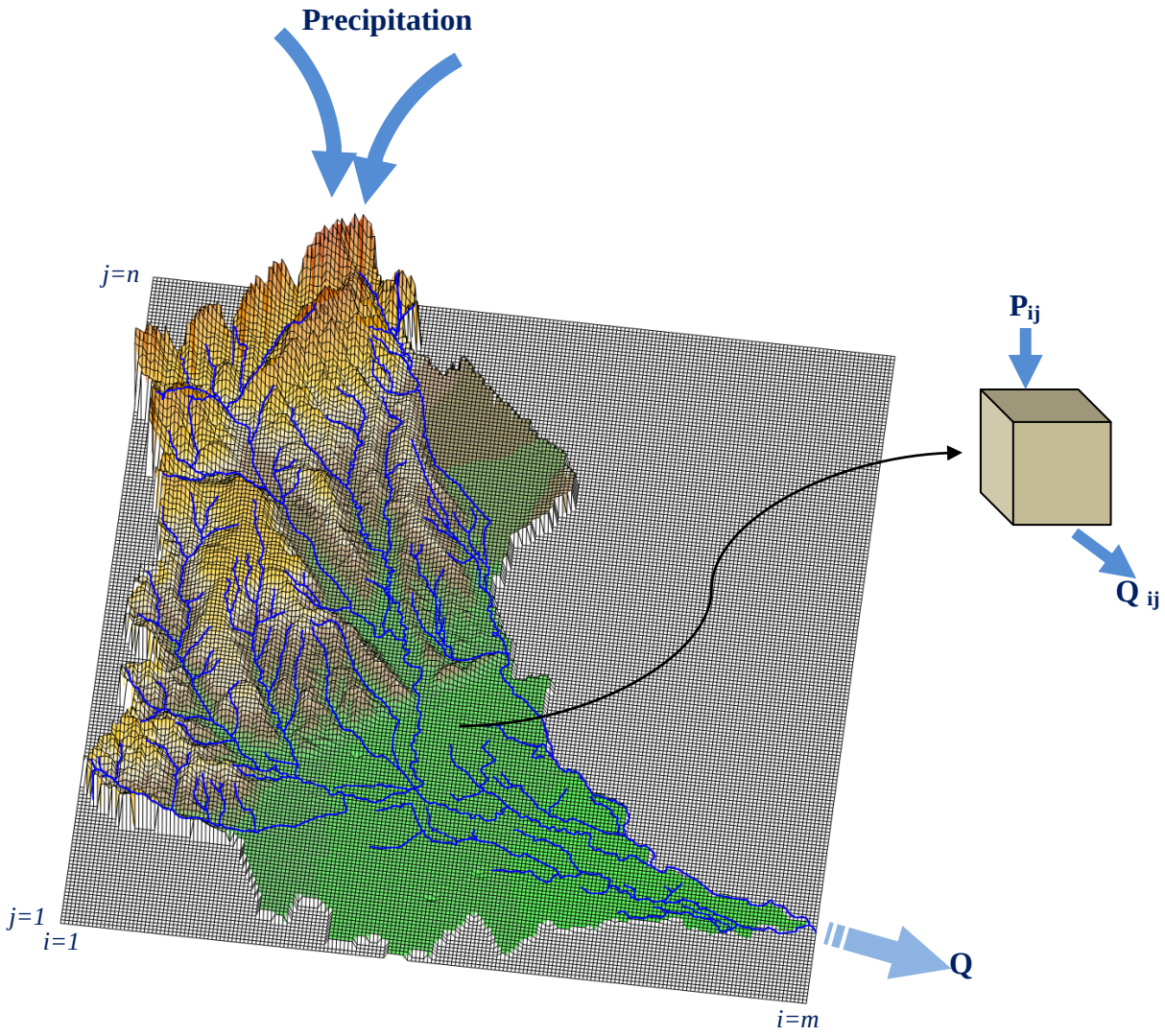

Figure 1.1. Schematic diagram of a distributed model. The model accounts for each grid cell of the basin.

The semi-distributed and distributed models take an explicit account of spatial variability of processes, input, boundary conditions, and/or watershed characteristics. Of course, a lack of data prevents such a general formulation of distributed models, that is these models cannot be considered fully distributed (Melone et al., 2005). In particular, in the semi-distributed model (Fig 1.2) the above quantities are partially allowed to vary in space by dividing the basin into a number of smaller sub-basins which in turn are treated as a single unit (Boyle et al, 2001; Corradini et al. 2002; Todini, 1996).

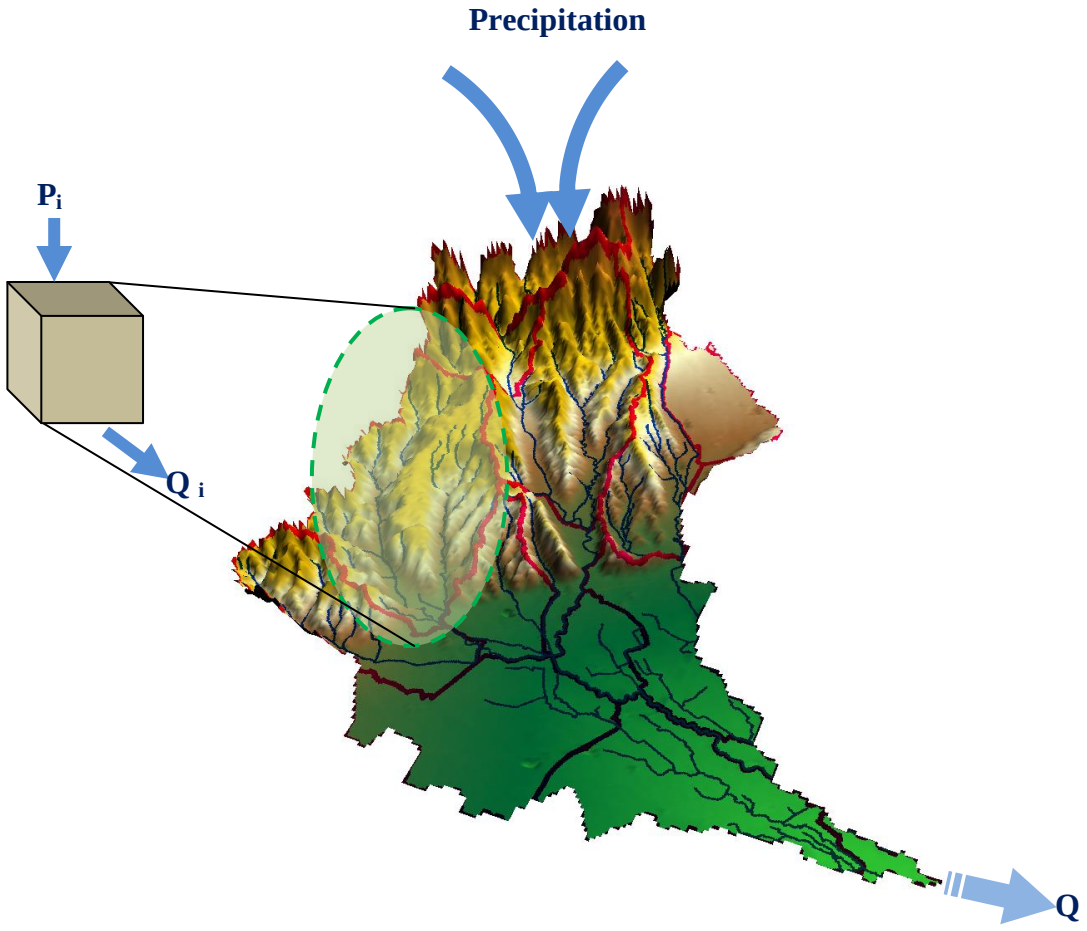

Figure 1.2. Schematic diagram of a semi-distributed model. The model accounts for each subcatchment of the basin.

Lumped models describe the watershed as a single unit with a homogeneous rainfall input (spatially averaged rainfall). In this type of models a uniform dynamics is considered to describe the discharge at the outlet (Fig. 1.3). Numerous lumped hydrologic models are

developed to simulated the watershed discharge. These models are usually based on the concept of the unit hydrograph (UH).

Regarding the temporal description rainfall-runoff model can be used to simulate a short time event or a continuous long time process. The first are designed to simulate individual rainfall-runoff events and their emphasis is placed on infiltration and surface runoff. The second model take explicitly account of all runoff components with provision for soil moisture redistribution between storm events (Melone et al., 2005).

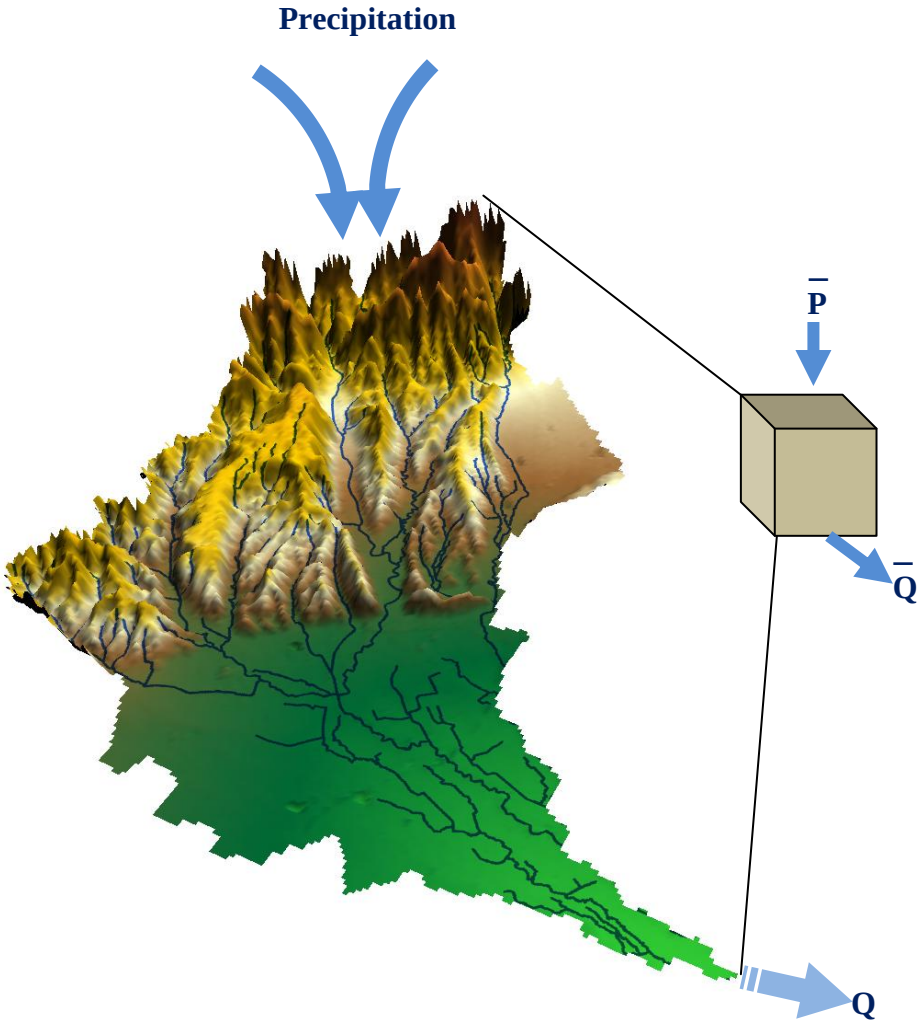

Figure 1.3. Schematic diagram of a lumped model. The model accounts for the entire basin as a single unit.

The selection of a particular model is a key issue to get satisfactory answers to a given problem. Although there are no clear rules for making a choice between models, some simple guidelines can be stated. Starting from the studied physical system, the first step is to define the problem and determine what information is needed and what questions need to be answered. This means that it is necessary to evaluate the required output, the hydrologic processes that need to be modelled, the availability of input data. Subsequently the simplest method that can provide the answer to the questions has to be chosen. In particular, it is necessary to identify the simplest model that will yield adequate accuracy, bearing in mind that model complexity is not synonymous with the accuracy of the results. The model has to be characterized by flexibility, by the possibility of making it applicable under various spatial and temporal conditions and that increased accuracy has to be worth the increased effort (Lastoria 2008). A possible methodology for selecting a rainfall-runoff model is proposed by Anderson and Burt (1985) and showed in the figure 1.4 (Perrin et al., 2002).

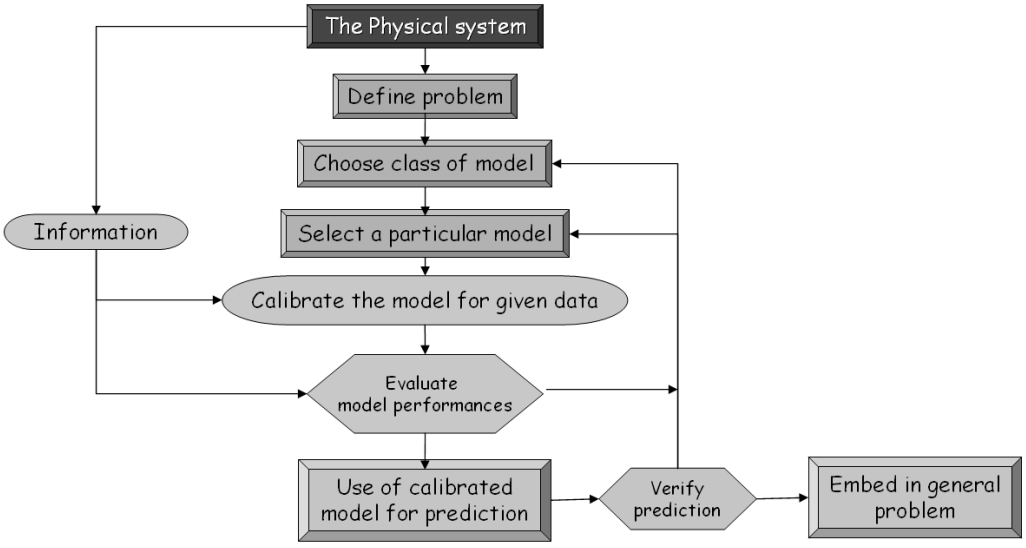

Figure 1.4. Rainfall-runoff model selection diagram according to Anderson and Burt (1985).

A rainfall-runoff model has different components as input:

- Topographic data
- Geomorphic data

- Meteorological data

The topographic information plays an essential role. It is an important land-surface characteristic that affects most aspects of water balance in a catchment, including the generation of surface and sub-surface runoff, the flow paths followed by water as it moves down and through hillslopes and the rate of water movement (Vaze and Teng 2007). In the hydrological models the topography is represented by Digital Elevation Model (DEM). The physiographic information of the basin such as channel network, drainage divides; channels length, slope, subcatchment and catchment boundary are driven from DEM. Therefore, the quality and resolution (accuracy) of DEM affects the accuracy of above-mentioned hydrological features (Kenward et al., 2000).

DEM can be generated using two methods:

- By use of traditional methods such as classical topography (obtaining a cloud of points and lineal elements by means of direct measurement) or (and) photogrammetric techniques. Both systems have shown to be very reliable to date, obtaining DEMs that can be used for the definition of hydrologic models. These methods have technical or economical disadvantages.
- By use of Light Detection and Ranging (LiDAR) system which can provide accurate elevation data for both topographic surfaces and above-ground objects. It is an airborne optical remote sensing technology that measures scattered light to find range and other information on a distant target. This technology allows the direct measurement of three-dimensional structures and the underlying terrain.

DEM derived from traditional methods has a resolution greater than 25 m while the resolution of DEM derived from LiDAR measurements can be equal or greater than 1 m. With a low resolution DEM we may lose some physical information of terrain surface.

A common problem in determining flow pathways in digital terrain analysis is the problem of sinks in the DEM (Beven 1997). A related problem is that of river grid squares, where the actual river width may be much less than the grid size (Quinn et al., 1995; Saulnier, 1996). The small channels may not easily represented in DEM, but have an important effect on runoff routing (Beven 1997).

In some cases like large catchments, modeling a low resolution DEM can be used, but how coarse can be the DEM? The grid size of DEM can be so large in relation to the length of hillslopes that keeps the physical information. However, is shown that a DEM generated by re-sampling the high resolution data source (such as LiDAR) has more detail and is more accurate comparing the DEM derived from a low resolution data source like conventional contour maps (Vaze and Teng 2007). Numerous studies have presented their results comparing the quality of DEM and hydrological features driven from different sources. Liu et al. (2005) had compared DEM and hydrological features driven from LiDAR and contour maps (Vicamp data source). A DEM with 20 m grid size is generated using Vicamp data set to compare with a DEM with the same resolution driven from LiDAR data. Again a DEM with 5 m resolution was generated to show the effect of the resolution on the results. They had shown that the hydrological features are very sensitive to both DEM accuracy and resolution (in Figures 3, 4 and 5 of their article). The elevation differences in two DEMs are significant and is about 65 meters in some area.

It is worth to note that the DEM derived from LiDAR data has a horizontal and vertical accuracy of 1.5 m and 0.5 m respectively, while the accuracy of conventional DEM is dependent to scale with vertical accuracy of the DEM is to within 0.5 of contour interval.

With LiDAR data, we can generate a high density and high accuracy DEM. High density data make it possible to represent terrain in much detail. However, millions and millions data point means a very high volume data sets. This imposes high performance storage and data analyzing hardware and software.

Geographic Information Systems (GIS) applications are powerful tools for display, store, analyze, retrieve, and process spatial data. Application of GIS in hydrological modeling has been developed during the last decade realizing the advantages of incorporating GIS with hydrologic modeling. Capability of managing large spatial data sets and analyzing the data to generate high resolution DEM and extracting hydrological features and data pre-processing (such as sink removing) encourages the hydrology community to integrate GIS applications with hydrological modeling. This linking is so strong that “GIS based hydrological modeling” is an interesting theme in hydrological modeling studies. Maidment (1996) summarized the different levels of hydrological modeling in association with GIS as follows: hydrologic assessment; hydrologic parameter determinations; hydrologic modeling inside GIS; and linking GIS and hydrologic models.

This study is aimed to simulate the response of Monticano River basin (Veneto, Italy) to different precipitation events. The rainfall-runoff model, TOPMODEL, is selected to apply for this study.

1.3. TOPMODEL

TOPMODEL (TOPography based hydrological MODEL) is a semi-distributed and partly physically based model. It is a topography based hydrological program and predicts the response of a single or multiple sub-catchments. It considers an average rainfall and potential evapotranspiration for the whole catchment (Narula et al., 2002). The main concept behind this model is to give detailed account of very important topographic and hydrologic features of a watershed. The TOPMODEL is developed on the basis that the catchment storage is related to the local water table in which the main factor is the topographic index (Beven and Kirkby, 1979).

The simplicity of the model comes from the use of the topographic index, $\kappa=\alpha/\tan\beta$, first introduced by Kirkby and Weyman (1974) and Kirkby (1975), where α is the area draining through a point from upslope and $\tan\beta$ is the local slope angle. This index, or the later soil topographic index ($\alpha/T_0 \tan\beta$) introduced by Beven (1986), is used as an index of hydrological similarity. All points with the same value of the index are assumed to respond in a hydrologically similar way (Beven 1997).

The topographic index of TOPMODEL is scale dependent, so that parameter values and consequent results are strictly dependent and sensitive to grid size or DEM resolution. For this reason the model requires a high quality DEM, without sinks. The recommended resolution of the grid size is not greater than 50 m (Lastoria, 2008).

TOPMODEL is mainly used to simulate humid or dry catchment responses, predicting flood frequency.

TOPMODEL is defined as a variable contributing area conceptual model in which the dynamics of surface and subsurface saturated areas is estimated based on storage discharge relationships established from a simplified steady state theory for down-slope saturated zone flows. The theory assumes that the local hydraulic gradient is equal to the local surface slope and implies that all points with the same value of the topographic index, will respond in a hydrologically similar way (Lastoria, 2008).

1.4. Motivation of the study

The objective of this study is to apply the rainfall-runoff hydrological model, TOPMODEL (modified version of the Department of Civil and Environmental Engineering, University of Trieste) to the Monticano river basin, located in the Province of Treviso, Veneto, Italy.

This work has two main goals:

- Flood prediction
- Determining the effect of LiDAR driven DEM on the topographic index and the model results

The ability of the model to describe the immediate responses of Monticano River to high intensity of rain events is determined.

The availability of the high resolution LiDAR data of the study area enabled us to generate a high quality DEM using the GIS applications. The hydrological features of the basin are extracted from generated DEM.

TOPMODEL is sensitive to topographic index distribution, and the topographic index is a function of the DEM resolution. To determine the effect of DEM resolution on the results of the model, DEMs with 25 m, 50 m, 100 m and 200 m grid size are generated from the high resolution data source to calculate the topographic index and topographic index distributions.

The efficiency of the model is evaluated to explain the quality of the model results.

Chapter Two

Background

2.1. Introduction

As introduced in chapter one, TOPMODEL is a semi-distributed and partly physically based model. It is a topography based hydrological program and allows single or multiple sub-catchment calculations with average rainfall and potential evapotranspiration inputs to the whole catchment (Narula et al., 2002). This model accounts for variability in the hydrological response of different areas of a catchment by using an index of catchment wetness based on topography (Lastoria 2008). This means that areas possessing the same value of the topographic index are assumed to have the same hydrological behaviour. The local topography index is defined as $ln\ (a/\tan \beta)$ where (a) is the draining area per unit contour length through a location in the catchment, and ($\tan \beta$) is the hydraulic gradient, i.e. the slope of the catchment surface at the same location. The topographic index of TOPMODEL is scale dependent so that parameter values and consequent results are strictly dependent and sensitive to grid size or DEM resolution. For this reason the model requires a high quality DEM, without sinks. The recommended resolution of the grid size is not greater than 50m (Lastoria 2008).

This chapter is aimed to present a brief discussion on the background theory of TOPMODEL and a detail of TOPMODEL can be find in Beven 1997, Beven et al., 1995 and Beven 2001.

2.2. Theory of TOPMODEL

TPMODEL is a partly physically based semi-distributed rainfall-runoff model. It is based on three main assumptions (Beven 2001):

- There is a saturated zone in equilibrium with steady recharge rate over an upslope contributing area *a*.
- The water table is almost parallel to the surface such that the effective hydraulic gradient is equal to local surface upslope, tan β.
- The transmissivity profile may be described by an exponential function of storage deficit, with a value of T_0 when soil is just saturated to the surface.

The third assumption can be described as:

$$T = T_0 e^{-D/m} \qquad (2.1)$$

where T_0 (m^2/h) is the lateral transmissivity when the soil is just saturated, D (m) is local storage deficit and m (m) is a model parameter.
The downslope saturated subsurface flow rate q_i, per unit contour length (m^2/h) at any point on the hillslope can be expressed by:

$$q_i = T_0 tan\beta e^{-D_i/m} \qquad (2.2)$$

where β is local value of slope.

Considering the first assumption, and assuming that there is a spatially homogeneous recharge rate *r* (m/h) entering the water table, the subsurface downslope flow per unit contour length q_i can be calculated by:

$$q_i = ra \qquad (2.3)$$

where a is the area of the hillslope per unit contour length (m^2) that drains through the point i. combining Eq. 2.2 and Eq. 2.3, we can solve for the water table depth:

$$D_i = -m\ ln(\frac{ra}{T_0\ tan\beta}) \quad (2.4)$$

By integrating Eq. 2.4 over the entire catchment area A that contributes to water table, we can obtain a relation for mean water storage deficit:

$$\overline{D} = \frac{1}{A}\sum_i A_i \left[-m\ ln(\frac{ra}{T_0\ tan\beta})\right] \quad (2.5)$$

where A_i is the area associated with the i point.

By using Eq. 2.4 in the Eq. 2.5 and assuming that r is spatially constant and $ln\ r$ may be eliminated:

$$D_i = \overline{D} + m\left[\gamma - ln(\frac{a}{T_0\ tan\beta})\right] \quad (2.6)$$

Where $ln(a/T_0\ tan\beta)$ is the soil-topographic index (Beven 1986b), and

$$\gamma = \frac{1}{A}\sum_i A_i\ ln(\frac{a}{T_0\ tan\beta}) \quad (2.7)$$

Areal average transmissivity can be calculated by:

$$\ln T_e = \frac{1}{A}\sum_i \ln T_0 \quad (2.8)$$

Rearranging Eq. 2.6 gives:

$$\frac{\overline{D}-D_i}{m} = -\left[\lambda - ln(\frac{a}{tan\beta})\right] + [lnT_0 - lnT_e] \quad (2.9)$$

where $ln(a/\ tan\beta)$ is topographic index and:

$$\lambda = \frac{1}{A}\sum_i A_i\ ln(\frac{a}{tan\beta}) \quad (2.10)$$

is a topographic constant (Beven and Kirkby, 1979) for the catchment.

The Eq. 2.9 is a relation between the catchment average deficit (water table depth) and local deficit at any point in terms of deviation of the local topographic index from its areal mean and deviation of logarithm of local transmissivity from its areal integral value. The relationship is scaled by the parameter *m*.

The Eq. 2.6 implies that points with the same topographic index values will have identical response in the catchment. Therefore, it is not necessary to perform calculations for all grid points in the catchment, but only for different values of the topographic index. The soil-topographic index can be considered as an index of hydrological similarity.

Evapotranspiration is calculated in TOPMODEL using:

$$E_a = E_p \frac{S_{rz}}{S_{Rmax}} \tag{2.11}$$

where E_p is potential evaporation, S_{rz} and S_{Rmax} are root zone storage (m) and maximum available root zone storage (m).

At any point of the catchment The flux of water entering the water table is q_v which can be estimated by (Beven and Wood 1983):

$$q_v = \frac{S_{uz}}{D_i t_d} \tag{2.12}$$

where S_{uz} is storage in unsaturated zone (m), D_i is the local saturated zone deficit due to gravity drainage (m) and t_d is mean residence time for vertical flow per unit deficit (s/m).

The catchment average water balance is the sum of all local discharges:

$$Q_v = \sum_{i=1}^{n} q_{v,i} A_i \tag{2.13}$$

where A_i area element associated with the topographic index class *i* (m^2).

The output of saturated zone is base flow, which can be estimated by summing subsurface flows along each of N stream channel reaches of length l:

$$Q_b = \sum_{1}^{N} l_i (T_0 \, tan\beta) e^{-D_i/m} \tag{2.14}$$

Combining with Eq. 2.6:

$$Q_b = \sum_i \; l_i a_i \, e^{-\gamma - \bar{D}/m} \tag{2.15}$$

As a_i is contributing area per unit contour length then:

$$Q_b = Ae^{-\gamma} e^{-\bar{D}/m} \tag{2.16}$$

where A is the total catchment area (m^2).

We can estimate the base flow in terms of the average catchment deficit:

$$Q_b = Q_0 e^{-\bar{D}/m} \tag{2.17}$$

where $Q_0=Ae^{-\gamma}$ is the discharge when average deficit is equal to zero.

For a pure recession with zero input, the solution 2.17 shows that discharge has an inverse or first order hyperbolic relationship to time:

$$\frac{1}{Q_b} = \frac{1}{Q_0} + \frac{t}{m} \tag{2.18}$$

The catchment average deficit before each time step is updated by subtracting the unsaturated zone recharge and adding the base flow calculated for the previous time step:

$$\bar{D}_i = \bar{D}_{i-1} + \left[Q_{b_{t-1}} - Q_{v_{t-1}}/A\right] \tag{2.19}$$

The Eq. 2.17 can be used to initialize the saturated zone at the start of a run. In the case of given initial discharge, $Q_{t=0}$, which is assumed to be only the result of drainage from saturated zone, we can rewrite the Eq. 2.17 as:

$$\bar{D} = -m \; ln(\frac{Q_{t=0}}{Q_0}) \tag{2.20}$$

Having $\bar{D}$, we can calculate local values of initial storage deficit using Eq. 2.6.

The time delay of runoff due to distance from outlet can be evaluated by (Beven and Kirkby 1979):

$$t_i = \sum_{i=1}^{N} \frac{x_i}{v^* tan\beta_i} \tag{2.21}$$

where x_i is the plan flow path length (m), β is the slope of the *i*th segment of the flow path and v^* is velocity.

Chapter Three

Materials and Methods

3.1. Study Area

The study area is located in the Treviso Province, Veneto Region, north Italy (Fig. 3.1). The basin is limited from south to 45 49 9.73 N (Mareno di Piave), from north to 45 59 35.90 N (Tarzo), from east to 12 26 8.06 E (San Vendemiano) and from west to 12 11 45.33 E (Refrontolo). The watershed is closed on an observation station somewhere around Fontanelle.

The area of the basin is 170.30 Km^2 With a perimeter of 111216 m. The altitude of the basin is between 19 m and 588 m from mean sea level (MSL), with an average altitude of 87 m from the MSL. The half of the area is flat and has agricultural land use. The elevation increases toward the northwest and goes up to the mountains.

The Monticano River with about 50 km length is the main cannel of the basin. In the agricultural part of the basin, there are many artificial small channels that are ignored in this study.

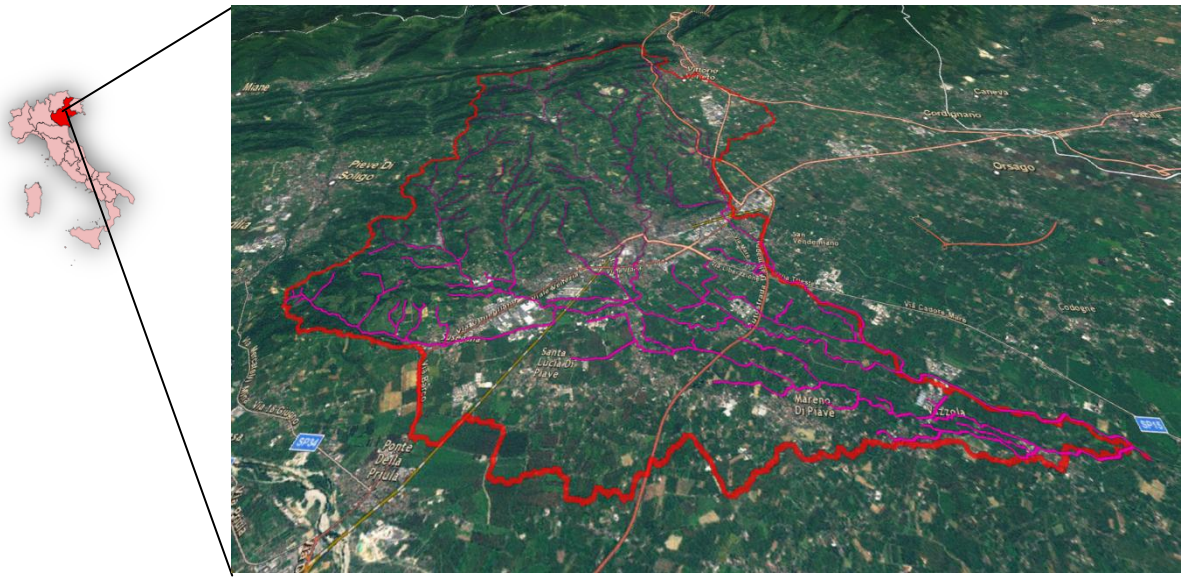

Figure 3.1. The panoramic view of the study area, Monticano basin, Monticano River and its streams.

3.1.1. Climate

The study area is located in the Veneto Region, so the area has the same climatological characteristics of this Region. The climate of Veneto Region has specific characteristics that are the result of combination of a set of factors that act at different scales. A key role is played by the position of the region, which is located in the middle latitudes. This causes the seasonal variations characteristic. In addition to previous reason, the Veneto is located in a transition zone between:

- Central European area which is influenced by the westerlies and large Atlantic Ocean fronts ("Cfb" climate according to Koeppen),

- South-European area where is influenced by subtropical anticyclones and the Mediterranean Sea ("Csa" climate, Koeppen).

The climate of Veneto is categorized into three main mesoclimate zones (Fig 3.2):

- Plain zone
- Alpine foothills zone
- Alpine zone

The plain mesoclimate zone characterizes the flat area of the region between the coastline and the piedmont area including the Euganean and Berici Hills. This area is

characterized by a relatively cold continental winters and warm summers. The average annual temperature is between the 13 °C in the inland areas and 15 °C in the coastal strip (Fig. 3.3).

Rainfall is distributed fairly throughout the year with total annual average between 600 mm and 1100 mm (Fig. 3.3). The winter is drier than average, while the autumn and spring seasons are dominated by Atlantic and Mediterranean perturbations with important rainfall events. In the summer, storms are frequent often associated with hail, and rarely with tornadoes.

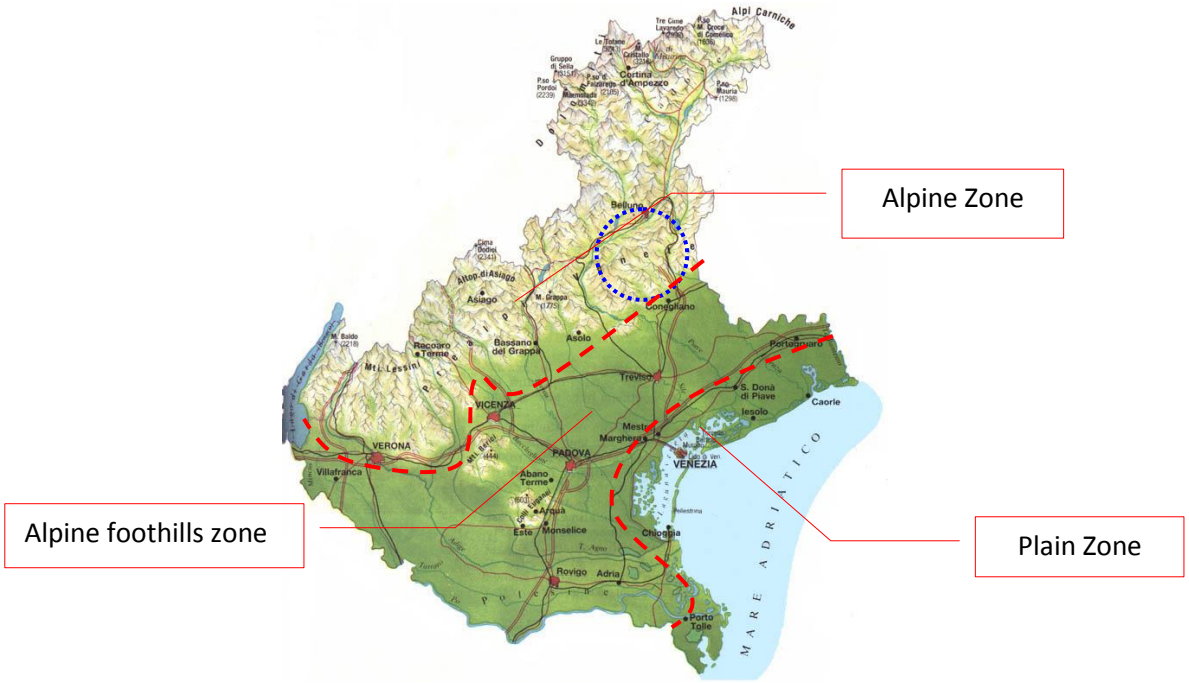

Figure 3.2. Veneto Region climate zones and, the study area is shown by dashed circle.

The Alpine foothills mesoclimate characterizes the area of pre-Alpine region and parts of the northern foothills, close to the mountains (Fig 3.2). The annual average temperature values of this areal range from 9-12 °C and the continentality is more important than the plain areas (Fig. 3.3). The winter is characterized by a higher frequency of days with clear skies and the relative scarcity of rainfall. The most striking feature of this zone consists in the abundance of precipitation, with annual average values between 1100-1600 mm, and a

maximum of 2000-2200 mm. The most important contributions are generally associated with spring and autumn.

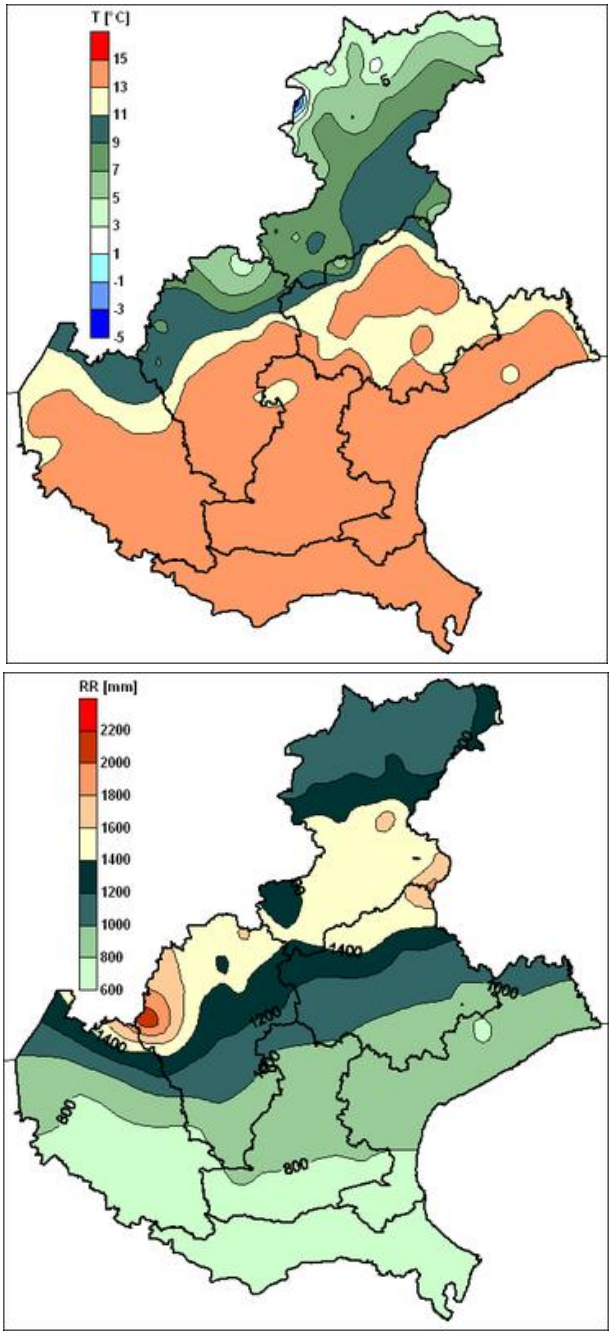

Figure 3.3. Average temperature (upper) and average precipitation (lower) in Veneto for the period of 1985-2009 (ARPAV, http://www.arpa.veneto.it/temi-ambientali/climatologia/approfondimenti/il-clima-in-veneto#RRmap).

The Alpine mesoclimate zone includes Dolomite mountain range, which is characterized by relatively high rainfall but generally less than 1600 mm per year, with maximum seasonal often in late spring, early summer and autumn (Fig. 3.3). The Average temperatures have values much lower than those of the Alpine foothills, with averages ranging from 7 °C to -5 °C and monthly mean values below zero in winter (Fig. 3.3).

3.2. Data

The data sets which are used in this study can be categorized in two main groups as follows:

- Topographic data
- Hydrological data

The data sets are acquired from different resources and various pre-processing are applied to them.

3.2.1. Topographic data

Topographic data coming from different resources are processed and combined to get the optimum results. The topographic data are used to create Digital Terrain Model (DTM), to delineate the watershed, to calculate topographic index, to investigate the study area and to perform some different steps in hydrologic processes. Different types of topographic data are used in each step, which are mainly:

- Topographic paper maps of scales 1:100000 and 1:10000
- Digital maps of scale 1:5000
- Satellite images
- LiDAR data

Satellite images from Google Earth service, classical paper maps of scales of 1:100000 (IGM) and 1:10000 along with digital maps of 1:5000 with more details (from Infrastruttura dei Dati Territoriali del Veneto, Regione del Veneto) are used to determine the study area and watershed delineation.

To generate the DEM of the basin the LiDAR data are used.

LiDAR is a distance measuring system based on lasers. For measuring the terrain features, an airborne LiDAR system is typically composed of sensor, Inertial Navigation System (INS) monitoring the pitch, roll, and altitude of the aircraft, and differential GPS receiving unit determining the location of the laser scanning system in three dimensional space (Hodgson et al., 2005, Barber and Shortrudge, 2004). A typical LiDAR system is illustrated in Figure 3.4.

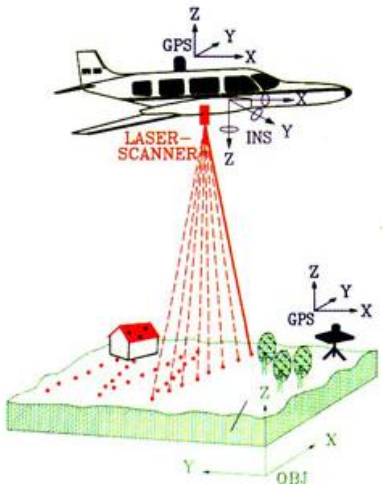

Figure 3.4. LiDAR system (Gross, 2003)

This technology allows the direct measurement of three-dimensional structures and the underlying terrain. Depending on the methodology used to capture the data, the resultant data can be very dense, for example, five points per meter. Such high resolution gives higher accuracy for the measurement of the height of features on the ground and above the ground. The ability to capture the height at such high resolution is LiDAR's principal advantage over conventional optical instruments, such as digital cameras, for elevation model creation.

The horizontal accuracy could be calculated as the flying height (usually 1000 m) multiplied by 1/2000. The vertical accuracy of cloud points can be within 0.1 meters and the horizontal accuracy within 0.5 meters if the density of cloud points is 1-5 per square meter (Lohr, 1998).

LiDAR data used in this study are obtained from project: “Rilievo LiDAR (laser a scansione) ed iperspettrale della Provincia di Treviso (Progetto Geo7)” by L’istituto nazionale di Oceanografia e Geofisica Sperimentale (OGS). For laser detection, the ALTM

GEMINI system was used, the system mounted in a helicopter (Ecureil AS350B2), owned by Helica srl di Amaro (UD). The LiDAR and hyper-spectral data have been elaborate by CARS group (Cartography and Remote Sensing), the Department of Geophysics of the Lithosphere of OGS.

3.2.2. Hydrological data

Hydrometric level data

Hydrometric level is measured with 30 minutes interval at Fontanelle hydrometric station (Fig. 3.5). The data set is provided by ARPAV (Agenzia Regionale per la Prevenzione e Protezione Ambientale del Veneto).

Figure 3.5. Hydrometric level measuring at Fontanelle station

The instrumentation on Fontanelle station includes:

- Hydrometric rod anchored against the left pylon of the bridge (Fig. 3.6 a). ARPAV has recently installed another rod in the same place to measure the lower water levels.

- An ultrasonic level gauge, equipped with the data transmission devices (as part of telemetry network of real-time hydro-meteo-pluviometric monitoring system of the Veneto Region) is installed downward on the bridge guard (Fig. 3.6 b). This instrument measures the water level with 30 minutes time interval.

Figure 3.6. a) Hydrometric rod and b) Tele-hydrometer at Fontenelle station

Discharge data

The discharge observation is performed using a current meter as well as an Acoustic Doppler Current Profiler (ADCP) at Fontanelle station by ARPAV.

An empirical function is introduced by ARPAV (2010) to convert the hydrometric level measurements to discharge values:

$$Q = 25.519 * (h + 0.02)^{1.611} \quad \text{for } h < +0.35\text{m} \quad (3.1)$$

$$Q = 21.064 * (h + 0.06)^{1.58} \quad \text{for } h >= +0.35\text{m} \quad (3.2)$$

Where *Q* is discharge in m^3/s and *h* is hydrometric level in m.

Pluviometric data

Precipitation is measured on a half hour time interval at two stations namely Conegliano and Vittorio Veneto. The position of these stations are presented in table 3.1:

Table 3.1. Positions of Pluviometric station. Altitude is above mean sea level.

Station	Altitude from msl (m)	East	North
Conegliano	83	1754728	5086125
Vittorio Veneto	122	1756207	5097775

3.3. Methodology

3.3.1. Generation of Digital Elevation Model (DEM)

The LiDAR raw data covers all features on the terrain such as ground, trees, buildings, highways, power lines etc. To generate the DEM, we need only bare ground data. To obtain the bare ground data a series of post processing are needed to apply to the LiDAR cloud points. Various filters are developed to remove the undesirable points (Zhang et al., 2003, Axelsson, 1999, Lin, 1997, Lee and Younan, 2003) to achieve the final cloud points for DEM generation. However, none of automated filter processes is 100% accurate so far. Manual editing of the filtering results is still needed. LiDAR data used for this study were classified into bare-ground and non-ground points.

The ArcGIS software is used to generate DEM in different steps. Here these steps are explained briefly. However, in the first step we need to create a geodatabase to save generated features in it.

LAS to multipoint

LiDAR data file is a very dense collection of points over the considered area, known as point clouds. Each file includes millions of points. These files were loaded into the geodatabase to save as multipoint format. The multipoint format has the advantage that

each record can save 3500 points instead of one point in the normal format. These data can be used to create a raster map. Due to filtering of data there were gaps in the spatial coverage, so holes or NULL values will appear in the map.

Geodatabase Terrain

A geodatabase terrain is generated to have an optimal estimation of the ground surface. The geodatabase terrain derives a triangulated irregular network (TIN) surface based on the classified points and systematizes the data for the fast retrieval (Fig. 3.7). The geodatabase terrain is the most efficient method for the maintaining the LiDAR data for the future applications. It can be edited even in locally and can be regenerated for the edited area.

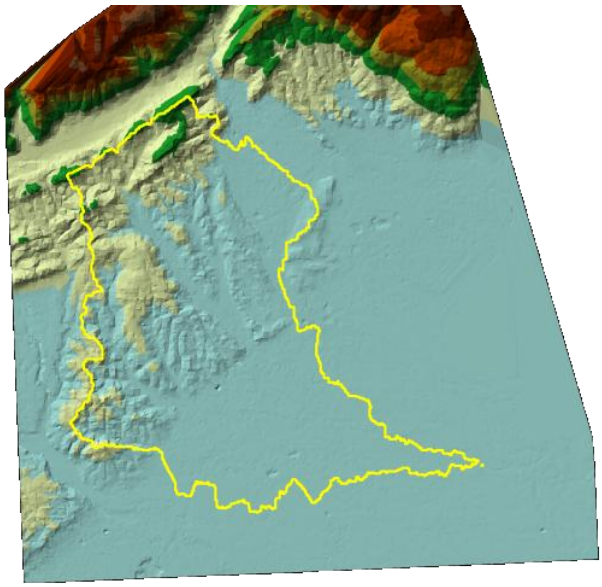

Figure 3.7. Geodatabase terrain derived from LiDAR data for the study area. The yellow line is the basin border.

Building DEM

The geodatabase terrain is used to generate DEM with desired resolution. The LiDAR data resolution is about 2 points per meter square, so it was possible to create a very high resolution DEM with at least cell dimensions of 2m×2m. As suggested by the model developer, the optimum DEM resolution for the TOPMODEL application is about 50 m. So a raster DEM with 50 m was created (Fig. 3.8). However, DEMs with 200 m, 100 m and 25 m were generated for comparing the resolution effect on the model results.

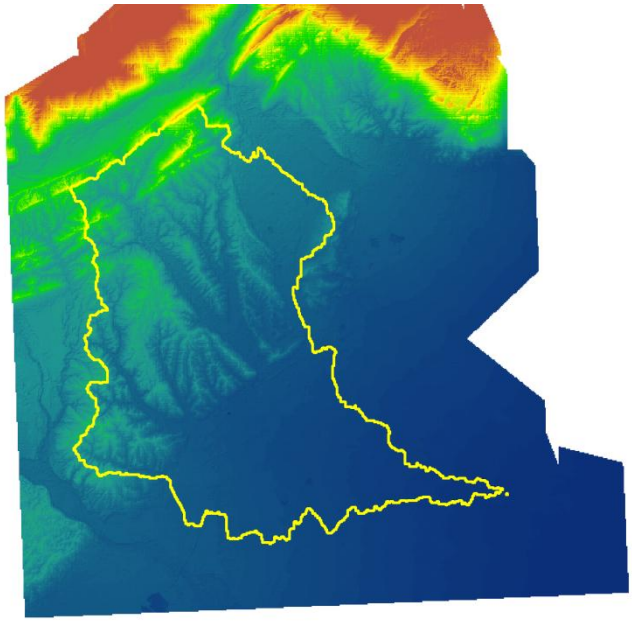

Figure 3.8. Raster DEM with 50 m resolution. The yellow line is the basin border.

3.3.2. Watershed delineation

The first step of preparing data for the hydrological modeling is watershed and streams delineation. Both of these data can be extracted from raster DEM provided in the previous section. The raster DEM generated from LiDAR data has more accurate elevations with respect to DEM derived from traditional methods. Consequently, the watershed boundaries can be extracted with more accuracy. This procedure is carried out applying ArcHydro tools (provided for ArcGIS) to the generated DEM as demonstrated in the Fig. 3.9.

DEM reconditioning

The main stream network (linear feature) provided by ARPA Veneto is used to modify the raster DEM. This modification is like to burning the stream network onto the DEM to be more evident in the next steps.

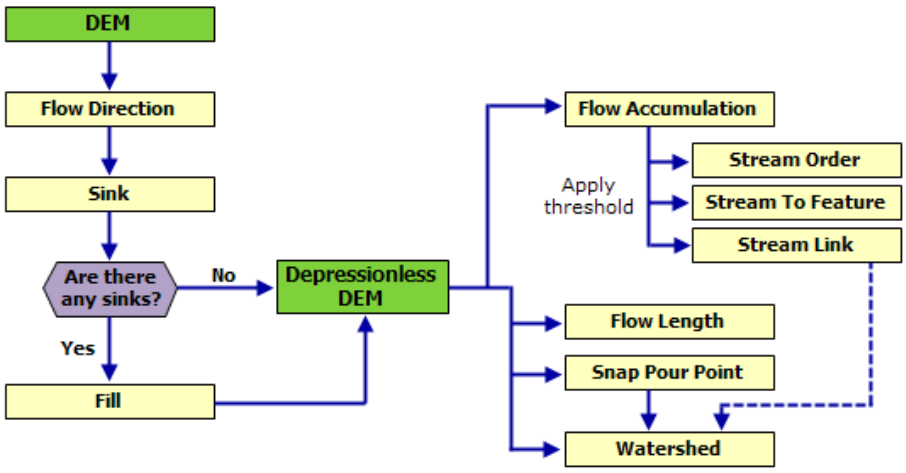

Figure 3.9. Procedure of watershed delineation (from ArcGIS 10, ESRI)

Flow direction

One of the keys to deriving hydrologic characteristics of a surface is the ability to determine the direction of flow from every cell in the raster. We need to create a raster of flow direction from each cell to its steepest downslope neighbor. The values for each direction from the center is shown in Fig. 3.10 (direction coding).

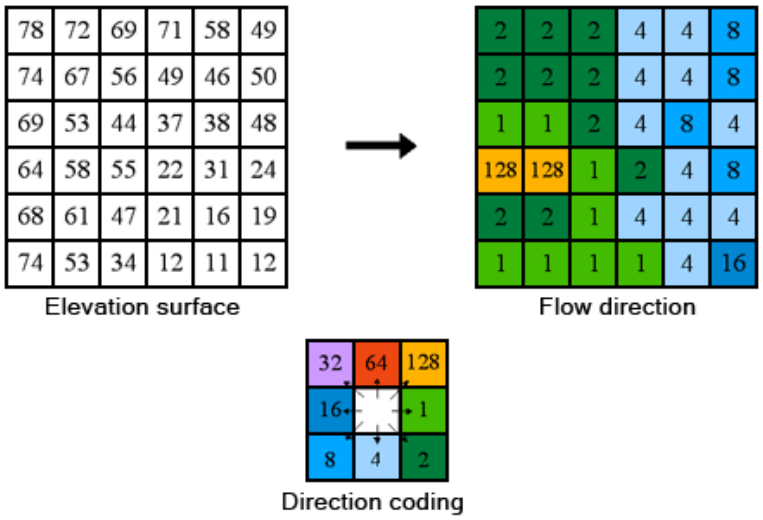

Figure 3.10. Flow direction determining of DEM (from ArcGIS 10, ESRI)

The flow direction map is an integer raster map with the same dimensions of the DEM. The flow direction map of the study area is shown in Fig. 3.11.

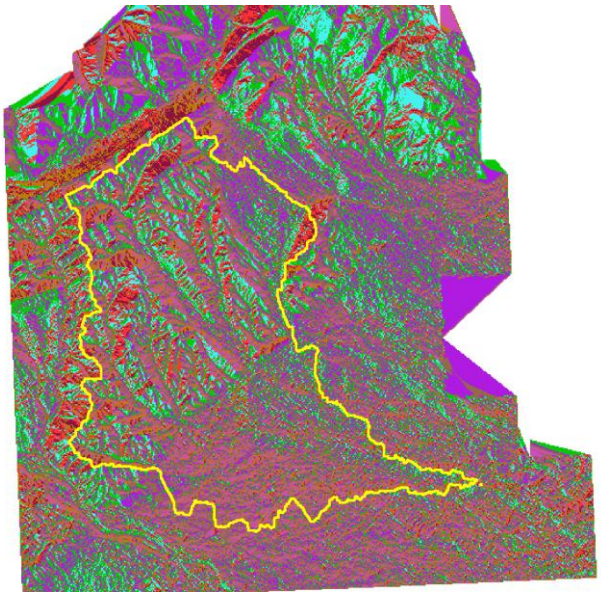

Figure 3.11. Flow direction map of study area. The yellow line is the basin border.

Fill sinks

A sink is a cell with an undefined drainage direction (Fig. 3.12). Its elevation is less than surrounded cells, so there is no flow from the sink cell. The sink cell is fined using the flow direction raster. The elevation of sink is modified such as to eliminate this problem.

The determined sink cells for the 50 m resolution DEM (Fig. 3.13) were modified except pour point.

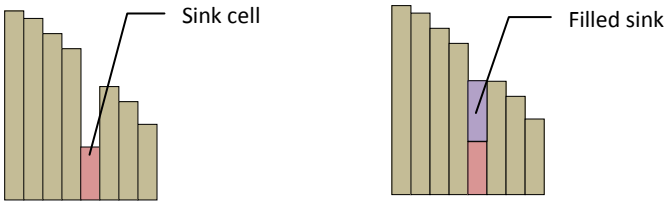

Figure 3.12. Profile view of a filled sink by modification its elevation

Flow accumulation

A flow accumulation grid consists of an integer value for each DEM point that represents the number of "upstream" DEM points whose flow path passes through it. High accumulation values indicate points in the stream, whereas low values represent areas of overland flow.

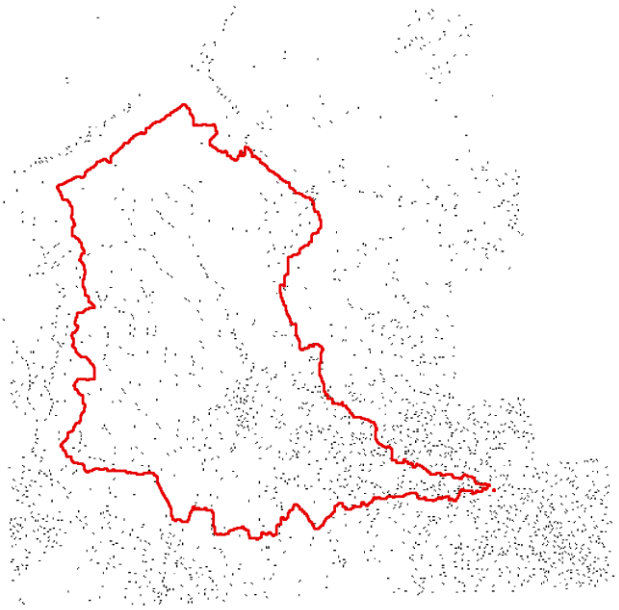

Figure 3.13. Sink cells of the study area

Cells of undefined flow direction will only receive flow; they will not contribute to any downstream flow. The relation between flow direction and flow accumulation is demonstrated in Fig. 3.14.

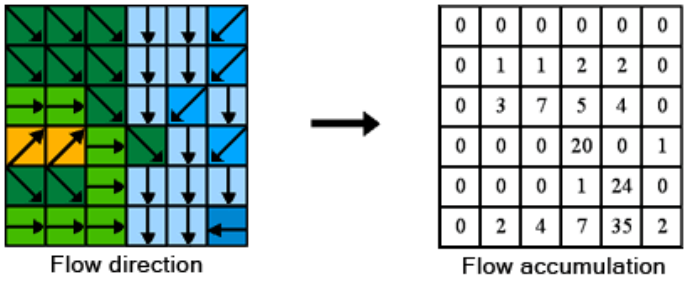

Figure 3.14. Flow accumulation determining (from ArcGIS 10, ESRI)

Stream definition

ARPA Veneto provided the main streams data as feature file. A more detail of the stream network was needed for defining the catchments and watershed. The value for river threshold is equal to 1% of the maximum flow accumulation. The determined stream network of the area is shown in Fig 3.15.

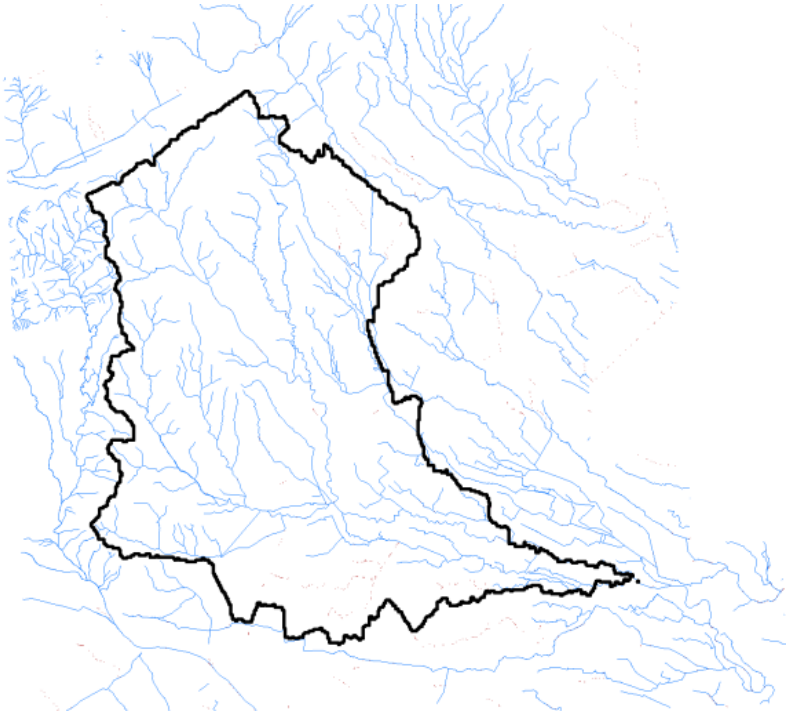

Figure 3.15. Stream network of the study area

Watershed delineation

Having the stream network and pour point, we can determine the sub-catchments (Fig. 3.16) and the watershed boundary.

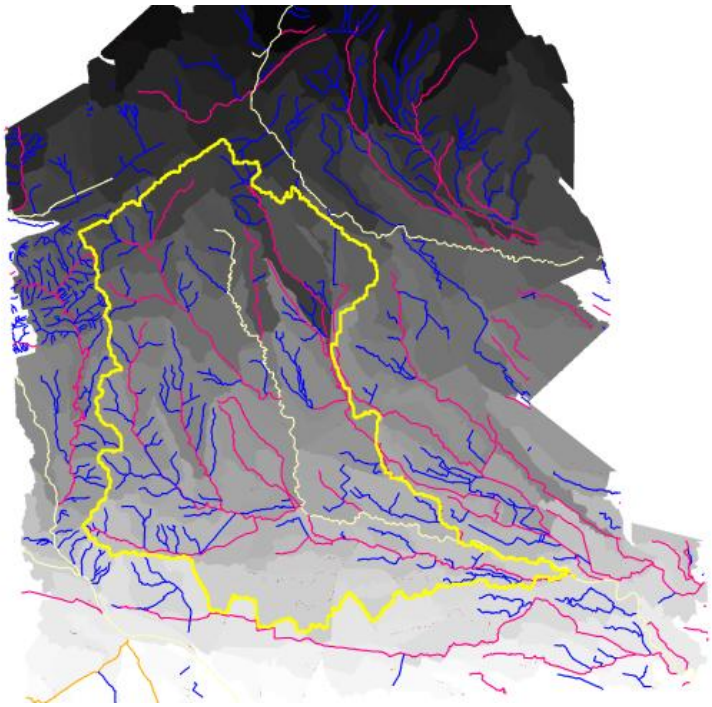

Figure 3.16. Stream network, sub-catchments and watershed boundary of the study area

Finally, we can mask the DEM and the stream network with the watershed boundary to have the exact basin (Fig. 3.17) for executing the model.

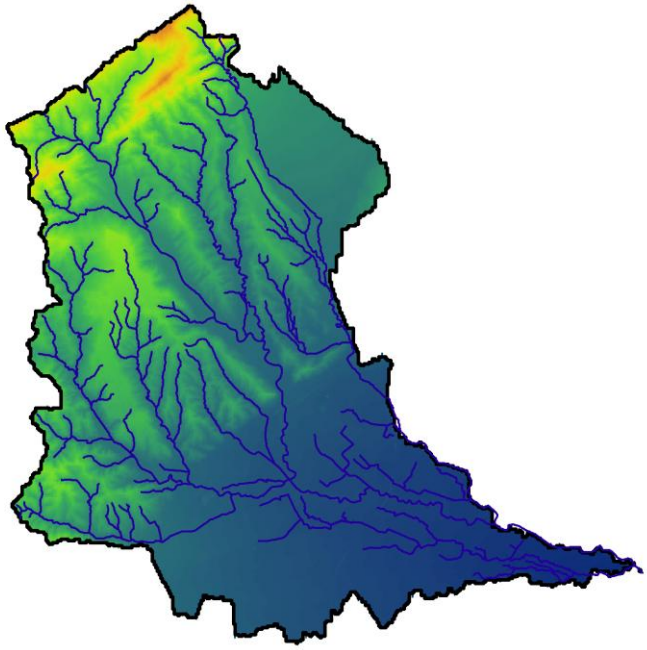

Figure 3.17. Watershed and stream network of the Monticano River.

3.3.3. Application of TOPMODEL to Monticano River basin

The theoretical background of the TOPMODEL is explained in chapter 2. In this section the parameterization of the model will be explained. These parameters were initialized and optimized in a repetition procedure to produce the flood predictions with minimum errors.

The inputs for the model are:

- Precipitation data
- Topographic index distribution
- Network width function
- Model parameters

These inputs and model parameters are prepared as explained in below.

Precipitation

The rainfall data were extracted for six events for the periods of 20-21 December 1997, 6-7 November 2000, 10-12 August 2002, 21-23 January 2003, 31 October-1 November 2004 and 22-26 December 2009. The rainfall data are measured in two meteorological stations in Conegliano and Vittorio Veneto. As in TOPMODEL the rainfall is considered spatially homogeneous, the measurements were interpolated over the basin applying the inverse distance weighted method:

$$p(x,t) = \frac{\sum_i \frac{p_i(t)}{d_i^2}}{\sum_i \frac{1}{d_i^2}} \qquad (3.3)$$

where $P_i(t)$ is the rainfall intensity at time t and position i and distance d from point x.

Topographic Index

The topographic index of the basin (Fig. 3.18) is calculated applying $ln\ (a/tan\ \beta)$ to DTM with 50 resolution. The distribution of the topographic index is prepared as an input for the model. As the topographic index plays a crucial role in TOPMODEL, to explain the effect of the resolution of DEM derived from LiDAR data on the results of model, the topographic index corresponding to DEMs with 25m, 100m and 200m cell size are calculated as well. The spatial distribution of the topographic index for each DEM resolution is calculated.

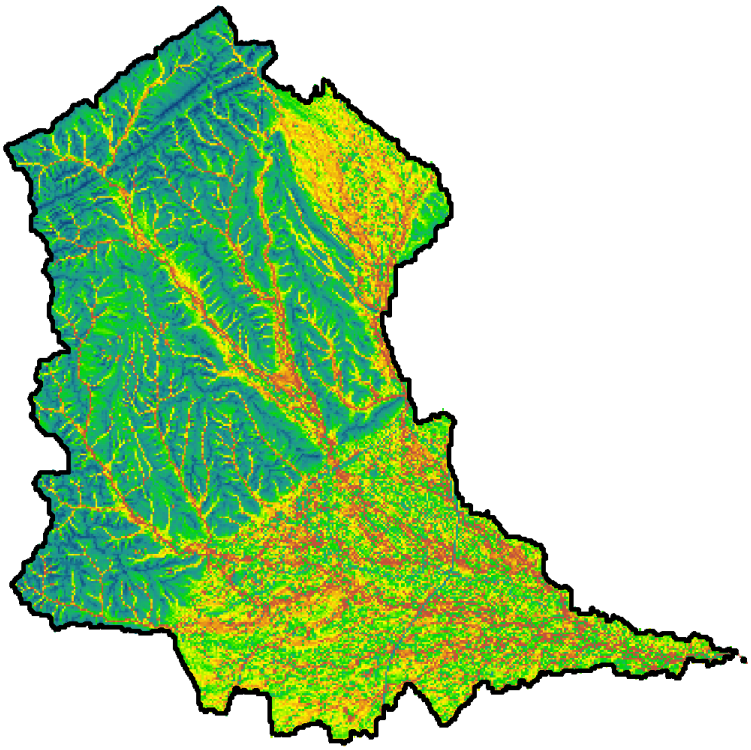

Figure 3.18. Topographic index (DEM with 50m resolution) of Monticano River basin

Network width function

The network width function is an important key indicator of geomorphic shape of the basin which describes channel development (Boggs et al, 2001). As it is correlated with the instantaneous unit hydrograph, it provides a good estimation of hydrologic response of the basin. The width function was calculated as the number of channels at successive distances away from the basin outlet as measured along the network (Surkan, 1968):

$$Z = \int_0^\infty N(x)dx \qquad (3.2)$$

The width function for the Monticano River basin is calculated on 250 m step size (Fig. 3.19).

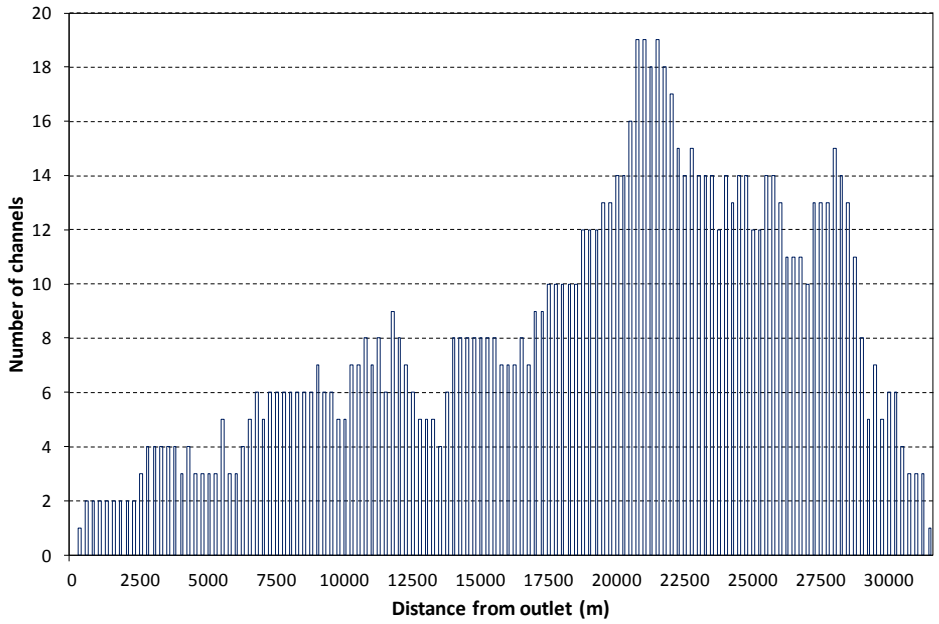

Figure 3.19. Network width function of Monticano River basin

Model parameters

The model parameters can be categorized into three groups:

I. Runoff generation parameters:

T_0	*Lateral Transmissivity at saturation D=0, $[L^2T^1]$*
m	*Scale parameter, decay constant of the transmissivity with the deficit [L]*
S_{Rmax}	*Field capacity of root zone [L]*
f_0	*Infiltration rate at t=0 $[LT^1]$*
f_c	*Infiltration rate at infinite time t=∞ $[LT^1]$*

II. Basin interior network dynamics:

C_G	*Wave speed of the flood, average in the basin $[LT^1]$*
D_G	*Diffusivity coefficient $[L^2T^1]$*

III. Principal network dynamics:

C_C	*wave speed of the flood, average in the principal hydrological network $[LT^1]$*
D_C	*Diffusivity coefficient $[L^2T^1]$*

T_0 is the lateral transmissivity when the soil is just saturated in:

$$T = T_0 e^{-D/m} \tag{3.3}$$

where T is transmissivity, D is local storage deficit below saturation and m is a model parameter controlling the rate of decline of transmissivity in the soil profile (Beven 2001).

S_{Rmax} is maximum available root zone storage which can be approximated by:

$$S_{Rmax} = Z_{rz}\left(\theta_{fc} - \theta_{wp}\right) \tag{3.4}$$

where θ_{fc} [-] is moisture content at field capacity and θ_{wp} [-] is moisture content at wilting point. For calibration, it is only necessary to specify a value for the single parameter S_{Rmax} (Beven 2001).

The parameters f_0 and f_c depend on the hydrological characteristics of the soil; in accordance with the classification of types of hydrological soil groups provided by the National Resource Conservation Service (NRCS). For the study area, the hydrological soil group is determined using the maps provided by ARPAV (Fig. 3.20). The f_0 and f_c parameters for Horton equation (Eq. 3.5-6) are extracted from corresponding table (Table 3.2).

Table 3.2. The parameters of Horton equation for different soil groups.

Hydrological soil group	***f₀*** ***[mm/h]***	***f꜀*** ***[mm/h]***	***k*** ***[1/h]***
A	200 – 250	12.5 – 25.5	2
B	125 – 200	6.5 – 12.5	2
C	76 – 125	2.5 – 6.5	2
D	25 – 76	0.25 – 2.5	2

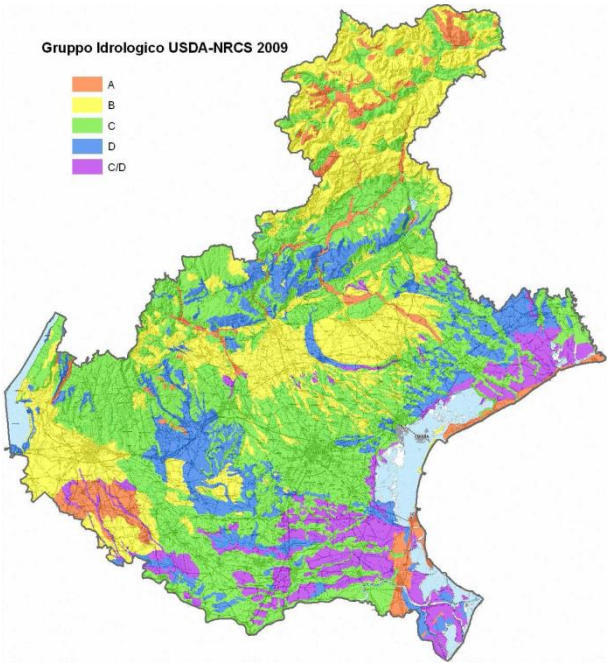

Figure 3.20. Hydrological soil group of Veneto Region (ARPAV 2011)

$$f(t) = f_c + (f_0 - f_c)e^{-kt} \quad (3.5)$$

$$F(t) = \int_0^t f(\tau)d\tau = f_c t + \frac{1}{k}(f_0 - f_c)(1 - e^{-kt}) \quad (3.6)$$

where f_0 is initial infiltration capacity (m/s), f_c is final infiltration capacity (m/s) and k is an empirical coefficient. f_0, f_c and k are a function of soil type.

The characteristics of the four soil groups; A, B, C and D are as follows:

***Group A**:* Soils in this group have low runoff potential when thoroughly wet. Water is transmitted freely through the soil.

Group B: Soils in this group have moderately low runoff potential when thoroughly wet. Water transmission through the soil is unimpeded.

Group C: Soils in this group have moderately high runoff potential when thoroughly wet. Water transmission through the soil is somewhat restricted.

Group D: Soils in this group have high runoff potential when thoroughly wet. Water movement through the soil is restricted or very restricted.

The wave speed of the flood can be estimated in a catchment by using (Beven 2001):

$$c = \frac{3}{2}v_0 \qquad (3.7)$$

where v_0 is the mean velocity at a reference discharge q_0 in a catchment of bed slop S_0 and Froude number F_0. These values are extracted from technical reports of ARPAV (2010b). Diffusivity coefficient is estimated by:

$$D_c = \frac{Q}{2B.f_f} \qquad (3.8)$$

where Q is discharge under the condition of full channel, B is channel width and f_f is average slope of the channel. This coefficient is estimated at 1000.

It should be noted that, in general, the coefficient of geomorphological dispersion is higher by about one order of magnitude compared to the hydrodynamic diffusion coefficient (M. Marani, Sulla funzione di ampiezza delle reti naturali, 1993).

Chapter Four

Results

The semi-distributed physically based hydrological model, TOPMODEL is applied to simulate the hydrological response of the Monticano River basin for selected events; 20-21 December 1997, 6-7 November 2000, 10-12 August 2002, 21-23 January 2003, 31 October-1November 2004 and 22-26 December 2009.

4.1. DEM and Topographic Index

The LiDAR data are used to generate DEMs with 25 m, 50 m, 100 m and 200 m (Fig 4.1). The hydrological features of the basin are derived from generated DEMs using GIS applications. As it is evident going from 25 m to 200 m grid size we lose some details as fine drainage network, slopes detail and maximum elevation. Clearly, the higher resolution has more details and corresponding hydrological features are more accurate. The statistics of the DEMs are presented in table 4.1. The sink cells are 2% of total cells for DEM with 50m, 100m and 200m resolution and a higher value of 6% for 25m grid size.

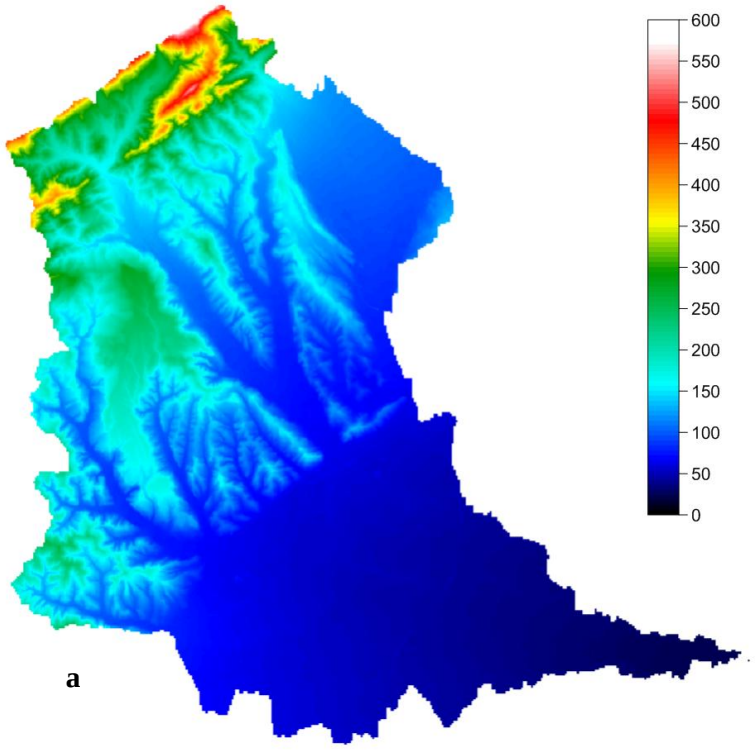

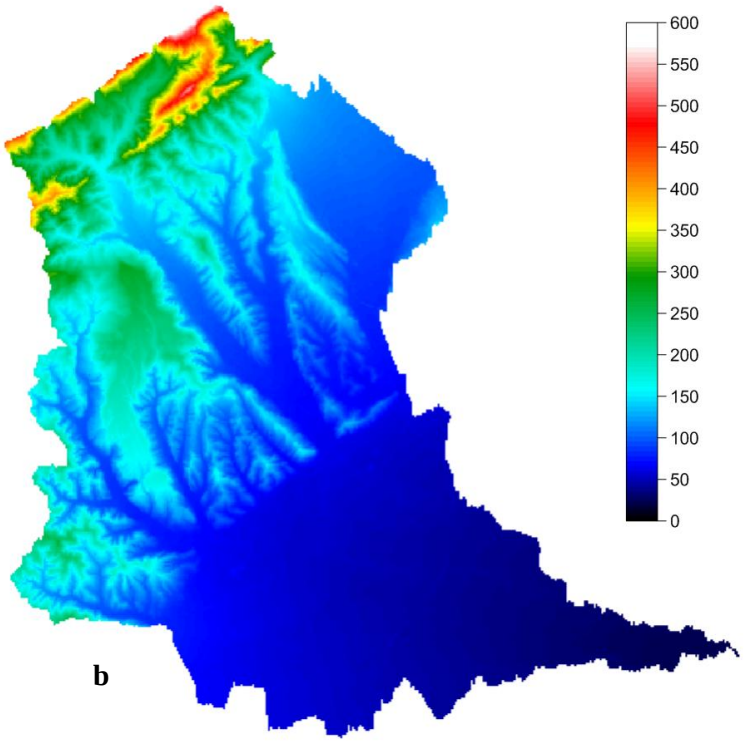

Figure 4.1. DEM with a)25 m, b)50 m, c)100 m and d)200 m grid size. Units are in meter.

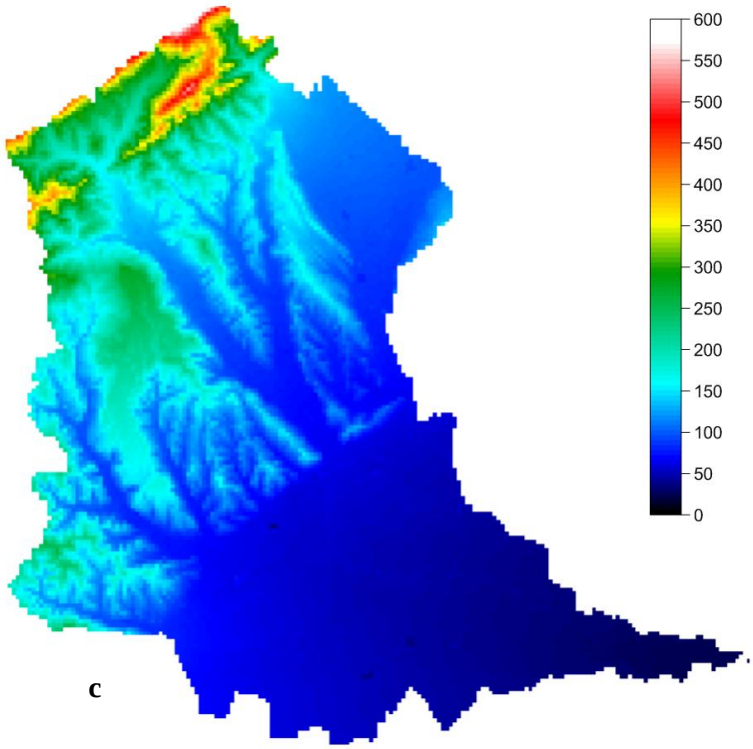

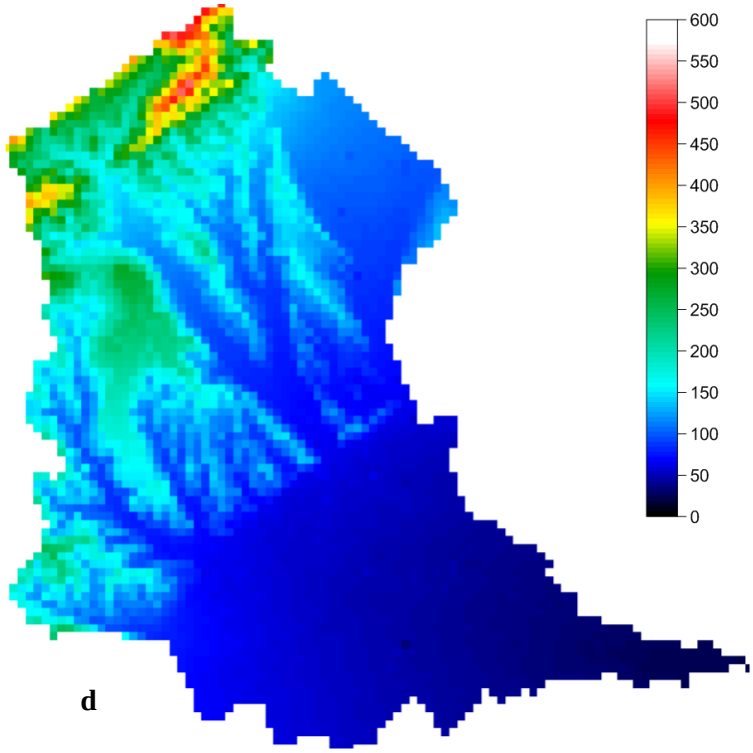

Figure 4.1. Continued.

Table 4.1. Statistics of elevation of DEMs with 25 m, 50 m, 100 m and 200 m grid size.

DEM Resolution (m)	Min (m)	Max (m)	Mean (m)	std	Cell count	Sink count
25	19.27	587.95	117.59	79.98	268316	16887
50	19.35	587.97	117.62	80.64	68145	1514
100	20.28	579.98	117.63	80.73	17018	243
200	20.83	518.48	116.18	78.67	4253	101

The generated DEMs are used to calculate the topographic index of basin (Fig. 4.2). The topographic index maps agreed well with subjective impression of the basin. The higher values of topographic index are corresponded to the area that tend to saturate first (Beven 1997) or in other words wet area which were found in the bottom of valleys which are potential subsurface or surface contributing area. The slopes have lower values. The index pattern indicates how the basin wets and dries. The spatial distribution of topographic index with 50 m grid size compared with real channel network (a combination of what provided by ARPAV and that derived from DEM), appear to be more realistic.

The corresponding distributions of topographic index are calculated. As it is evident in Fig 4.3, there is a distinct swift of topographic index density function toward higher values as the DEM resolution increases. This is because by increasing the DEM grid size the higher frequency topographic information is lost.

Some statistics of the topographic index of each resolution are presented in table 4.2. The topographic constant (Beven and Kirkby, 1979) as an indication of topographic characteristics of the basin is calculated by:

$$\lambda = \frac{1}{A}\int_A \ln\left(\frac{a_i}{\tan\beta_i}\right) dA \qquad (4.1)$$

where A is the basin area. By increasing the grid size of DEM, the values of topographic index constant increases (Table 4.2).

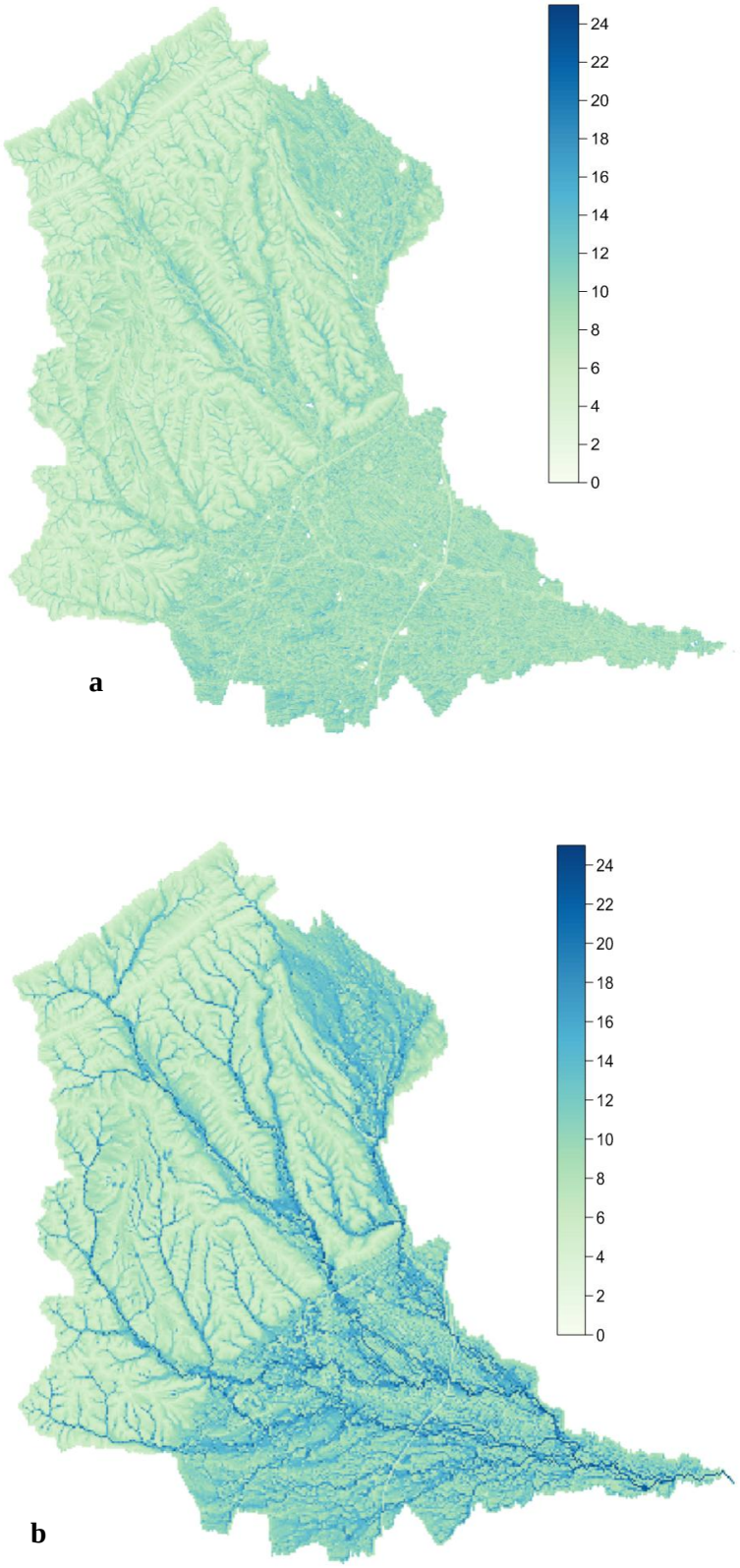

Figure 4.2. Topographic index map for a)25 m, b)50 m, c)100 m and d)200 m DEM resolutions

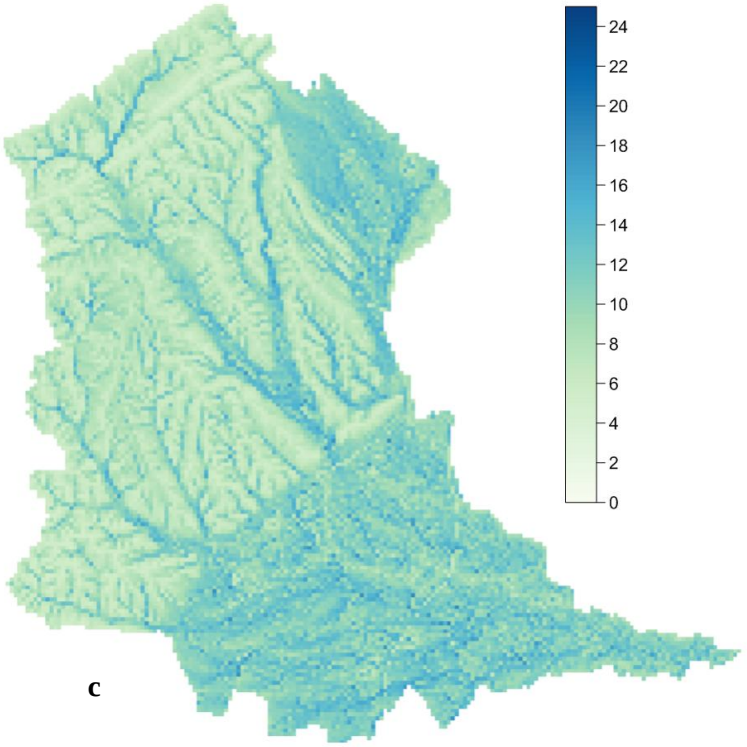

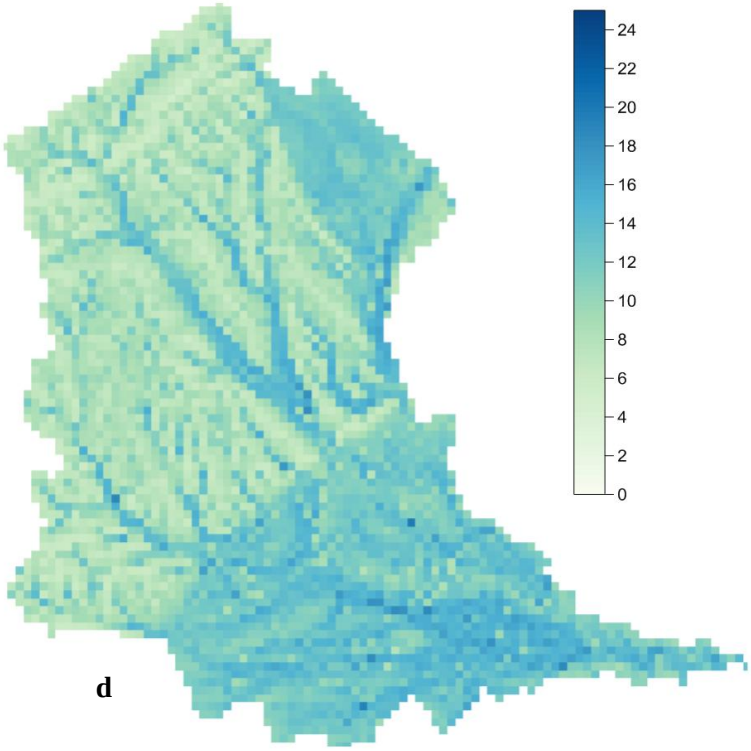

Figure 4.2. Continued.

Table 4.2. Statistics of topographic index derived from DEMs with 25m, 50m, 100m and 200m grid size.

DEM Resolution (m)	Min	Max	std	λ
25	2.26	20.67	2.23	7.36
50	3.12	24.83	3.93	9.19
100	4.02	18.86	2.70	9.23
200	5.00	19.85	2.83	10.32

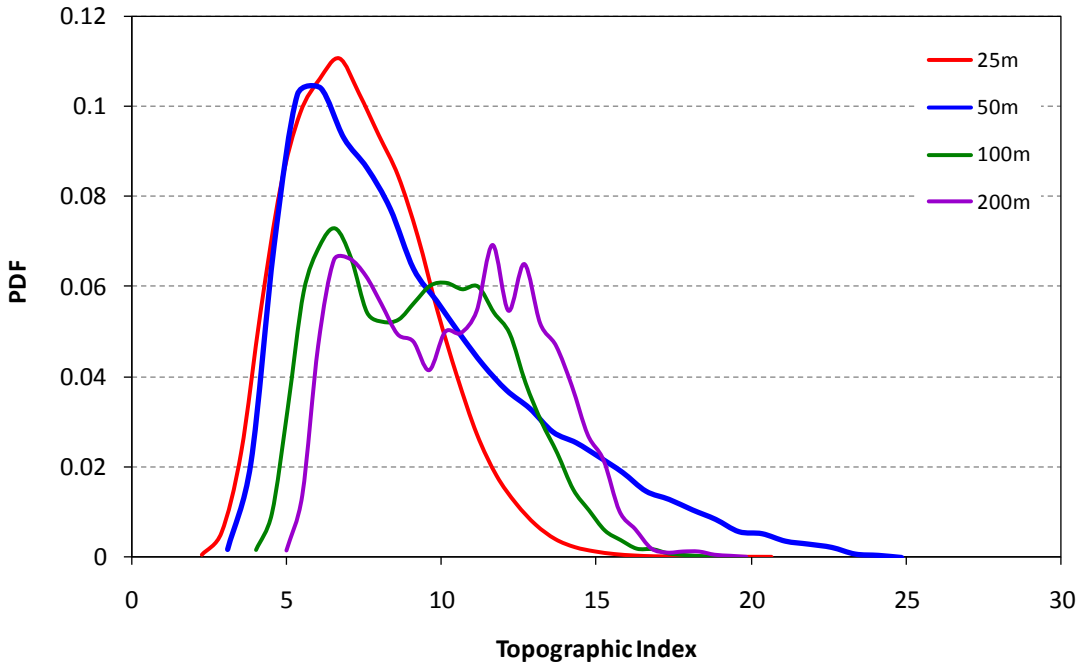

Figure 4.3. Effect of DEM resolution on the distributions of topographic index. The red, blue, green and violet lines are the distribution of topographic index driven from DEMs with 25m, 50m, 100m and 200m grid size respectively.

As it is shown in Fig. 4.3, the shape of topographic index distributions for 100m and 200m resolutions have significant difference with those of 25m and 50m grid sizes. The differences are mainly in the topographic index values of 6-10. To investigate the reason of this difference the maps of topographic index for low values and high values are generated. The lower values are representative for the slopes and peaks, while the higher values are representative for the valleys.

Moving from high resolution to low resolution, we lose some details of topographic features. For instance, once changing the grid size from 25m to 200m, every 64 cells are substituted with just one cell. Therefore, it is obvious that by considering one cell instead of 64 cells, especially in hill slopes and steep areas, the distribution of topographic index is affected significantly. The maps of topographic index values up to eight (lower values) for 50m and 200m grid size are shown in Fig. 4.4. The differences between two maps reveal that in topographic index based on DEM with 50m cell size cannot be a good representative of the characteristics of the area (Fig. 4.4b), while the topographic index with 50m grid size shows much details of the slopes and stream network which gives a better understanding of the wetting the basin.

The changing resolution affects the distribution of topographic index in the mountain area. Increasing the cell size causes to decrease the number of cells with e specific value of topographic index, in this case 6-7. Consequently, this affects the shape of distribution curve (Fig. 4.3).

In the same way, the higher values of topographic index are affected. By increasing the cell size, we lose details about the area that wet first, such as valleys. As shown in Fig. 4.5, the topographic index map based on 50m grid size gives very clear idea of stream network (which wets first) even the small branches of the network, while in the lower panel with 200m grid size we see only a shadow of main network. In the mountain area, the detail of network disappeared, in the flat area the routs are merged, and the stream network is not distinguishable from flat land.

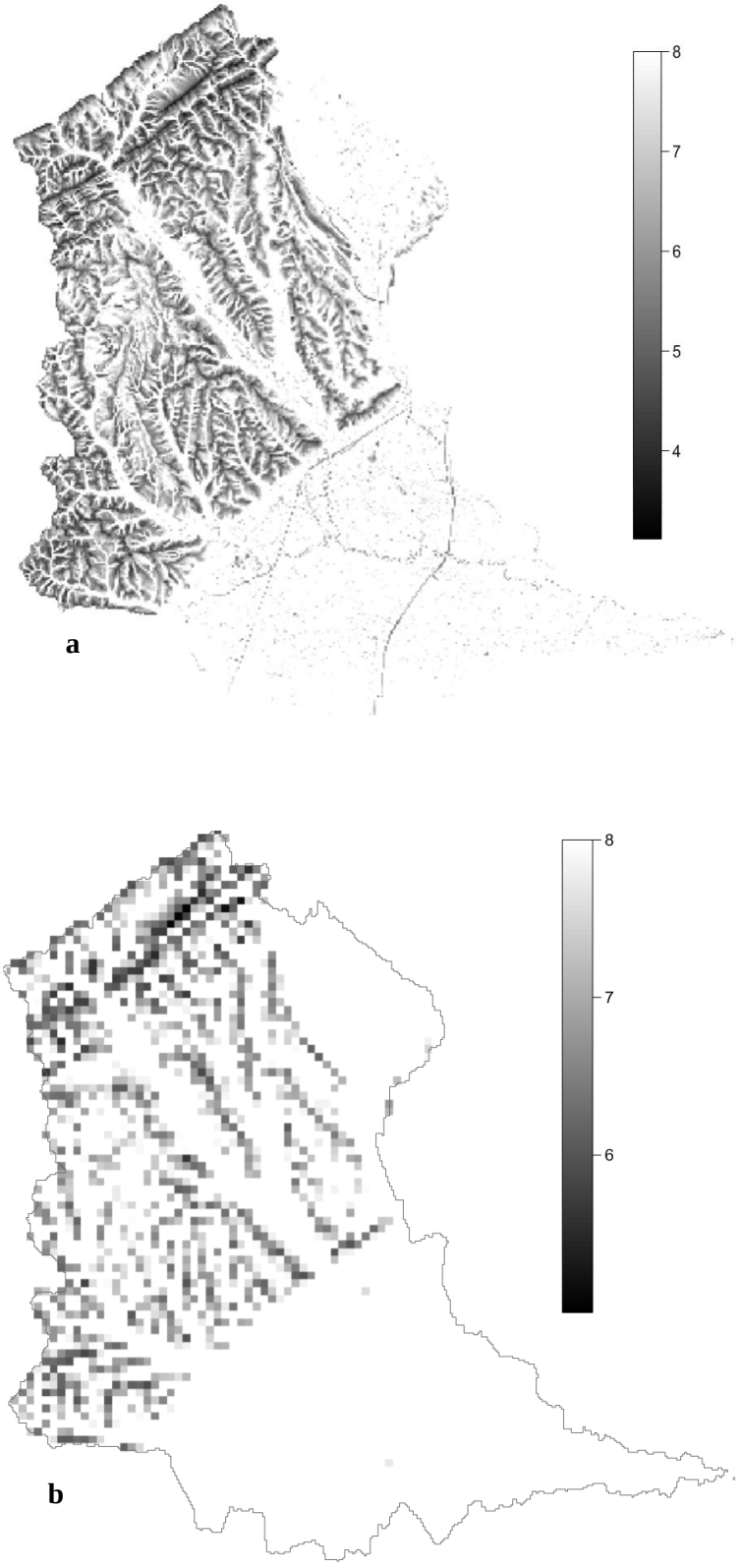

Figure 4.4. Topographic index map of small values up to 8, for a)50m and b)200m DEM resolutions

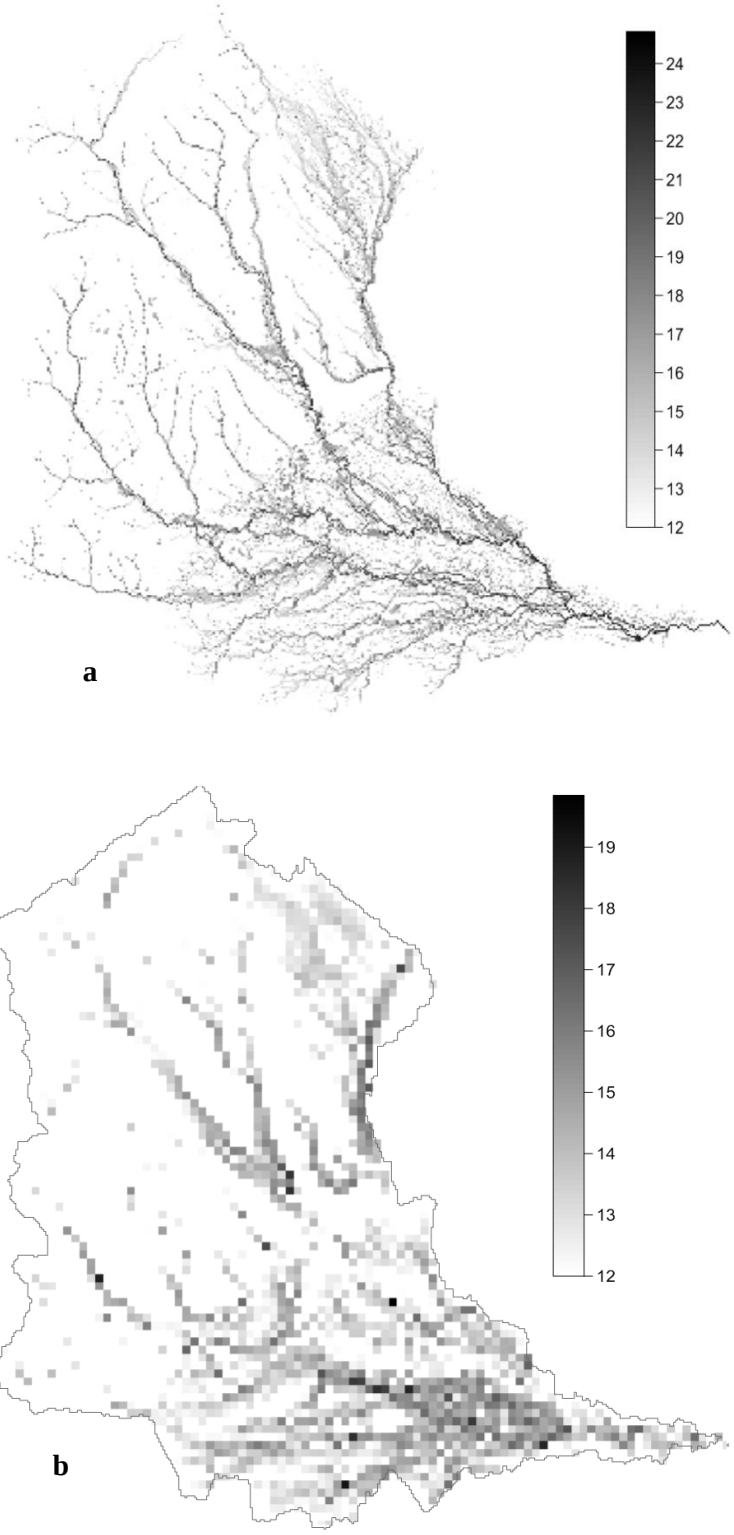

Figure 4.5. Topographic index map of larger values more than 12, for a)50m and b)200m DEM resolutions

4.2. Sensitivity Analysis

Of the model parameters, the variations of scale parameter *m* and lateral transmissivity T_0 have the important influence on the model performance. Other parameters such as field capacity of root zone, celerity of water are somehow deterministic, so investigating the sensitivity of model to variations of these parameters have no sense. Therefore, the effects of variations of these two parameters are determined. To highlight the impact of these parameters on the outcome of modeling, simulations were conducted with different values of T_0 and *m*. The sensitivity analysis results for event 2009 are shown in Figs 4.6 and 4.7. The simulated hydrograph corresponding to doubled and halved T_0 and *m* are compared with recorded hydrograph as well as with the simulation with optimum T_0 and *m* values.

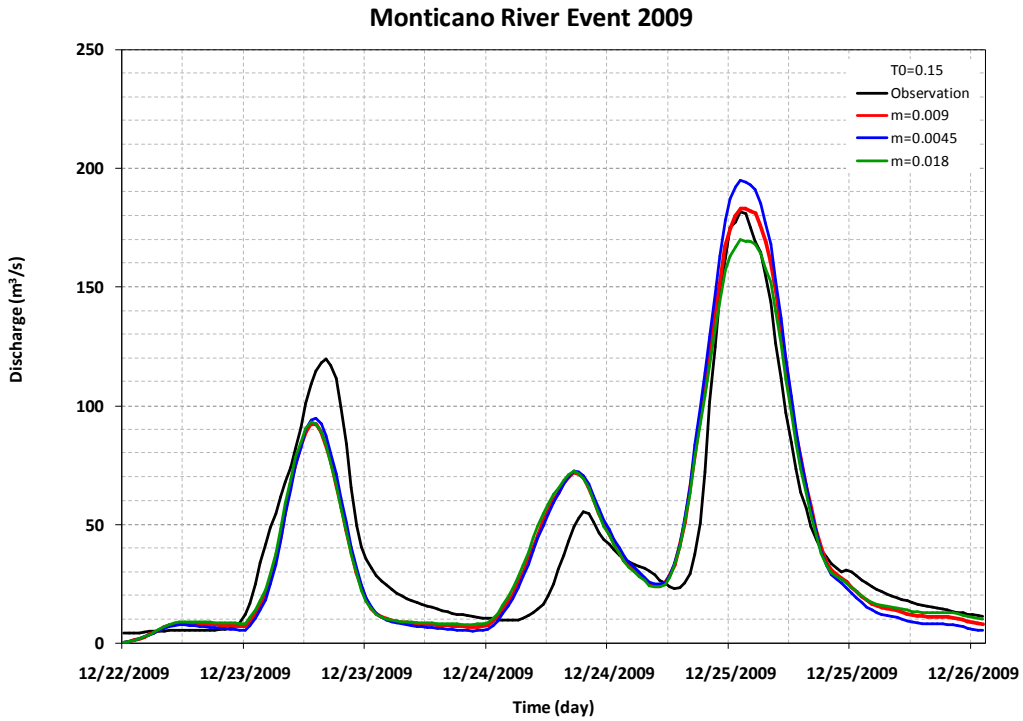

Figure 4.6. Sensitivity of model to scale parameter *m* for the event December 2009. The T_0 is fixes and *m* is variable. The black line is observation and red, blue and green lines are hydrograph simulations for *m* values of 0.009, 0.0045 and 0.018 respectively.

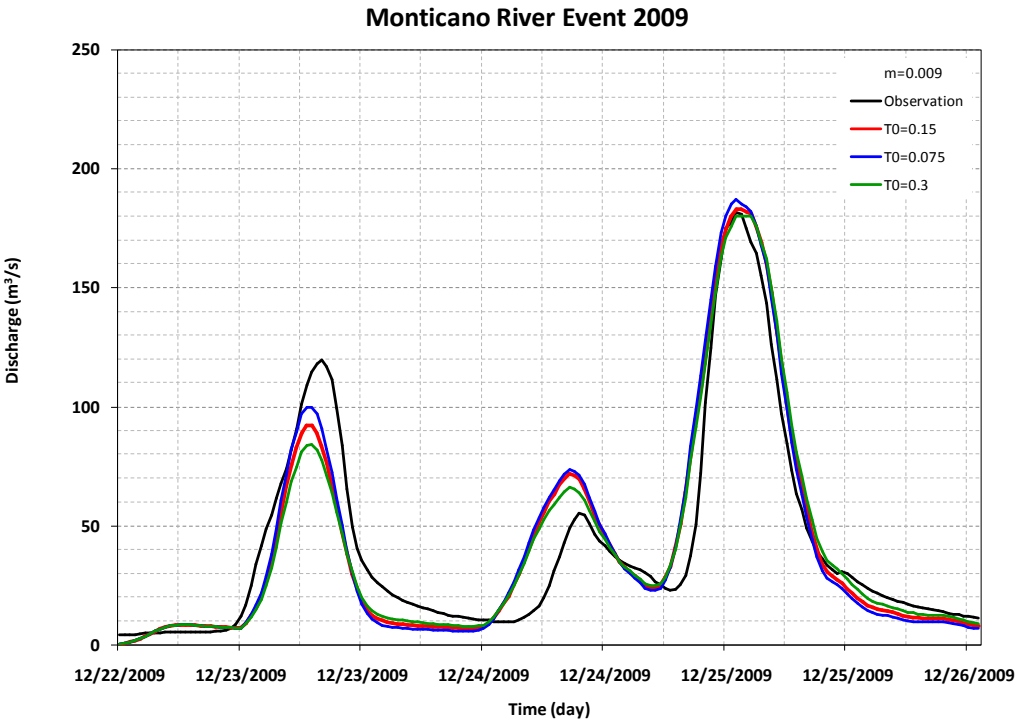

Figure 4.7. Sensitivity of model to T_0 for the event December 2009. The m is fixes and T_0 is variable. The black line is observation and red, blue and green lines are hydrograph simulations for T_0 values of 0.15, 0.075 and 0.3 respectively.

4.3. Model Calibration

The model parameters can be calibrated using observed stream flows from all events. Of the all parameters few ones are the main parameters with the most effect on the result that should be optimized to maximize the Nash-Sutcliffe efficiency (Nash and Sutcliffe, 1970). They are: scale parameter m, the saturated transmissivity T_0, the root zone parameter SR_{max} and for large catchments, the channel routing velocity v (Beven et al., 1995). These parameters are optimized by giving a small increment to each parameter and running the model for it. The results are used to create an optimization surface and the optimum values for the parameters are selected. The optimized parameters are presented in table 4.3.

Table 4.3. Calibrated parameters for hydrological simulation of Monticano River basin.

Parameter	**T_0 [m^2/h]**	**m [m]**	**SR_{max} [m]**	**f_0 [mm/h]**	**f_c [mm/h]**	**D_c [m^2/s]**	**C_c [m/s]**
	1.1	0.002-0.009	0.2	80	3	1000	1.5

4.4. Efficiency of Model

To check the goodness of the fit, the efficiency parameter of Nash and Sutcliffe (1970) is calculated for the simulation of each event based on:

$$E = 1 - \sum(Q_{obs} - Q_{sim})^2 / \sum(Q_{obs} - \overline{Q})^2 \qquad (4.2)$$

where Q_{obs}, Q_{sim} and $\overline{Q}$ are observation, simulation and observation average discharges respectively. The second term in the right hand side is the ration of error variance to variance of observations. The efficiency has a value equal to 1 with zero errors that means the simulation is equal to observation. It will be equal to 0 if he simulation would be equal to average discharge which means 'no-knowledge' model (Beven 2001). The negative values means even worse than 'no-knowledge' model.

Corresponding efficiency of each topographic distribution (based on different DEM resolutions) for each event is presented in table 4.4. The results show that in almost of the cases the efficiency corresponding to DEM with 25 m grid size is a bit higher than the others, except for event 1997. This means that the 25 m grid size can be used instead of a 50 m one. However, the efficiency may not be considered as a qualitative measure of the model performance.

Table 4.4. Efficiency of discharge simulation for Monticano River basin.

Event	**1997**	**2000**	**2002**	**2003**	**2004**	**2009**
Efficiency (DEM 25 m)	0.900	0.971	0.988	0.981	0.950	0.882
Efficiency (DEM 50 m)	0.904	0.971	0.982	0.966	0.945	0.882
Efficiency (DEM 100 m)	0.906	0.971	0.977	0.948	0.942	0.874
Efficiency (DEM 200 m)	0.908	0.971	0.967	0.910	0.932	0.857

4.5. Events Simulation

Event 20 December 1997

A 24 hours event with a maximum 210 m^3/s measured discharge, which is estimated with 90% efficiency. The peak value is well predicted, while the tails are underestimated. As shown in Table 4.4 and figure 4.9, the runoff volume is underestimated as well. The runoff to rainfall ratio (φ) for observation and simulation are 0.45 and 0.36 respectively.

Event 6-7 November 2000

This is a two days event, which is estimated with 97% of efficiency. The maximum discharge of 191 m^3/s is predicted by a value of 181 m^3/s. The total runoff volume is underestimated (Fig 4.10). The φ ratio for simulation is 0.38 versus 0.46 of observation.

Event 10-11 August 2002

The whole event is well predicted for both peak and total discharge values (Fig 4.11). The simulation efficiency is about 98%. The maximum discharge is 177 m^3/s, which is predicted with value of 176 m^3/s. The total runoff volume is well predicted with a φ ratio of 0.39.

Event 21-22 January 2003

The event is well predicted with a slightly shift of left tail (Fig 4.12). The efficiency of prediction is 97%. The total runoff volume is a slightly overestimated with φ ratio equal to 0.31. The measured peak value of 170 m^3/s is estimated at 167 m^3/s.

Event 31 October – 1 November 2004

This two days event is a little bit underestimated by an efficiency of 95%. The observed peak of 214 m^3/s is estimated at 210 m^3/s and the total runoff volume with φ ratio of 0.43 shows predicted values (Fig 4.13).

Event 22-26 December 2009

A four days event with three peaks, which is simulated with 88% efficiency and well runoff volume prediction (Fig 4.14). The maximum discharge has value of 181 m^3/s, which

is estimated as 183 m^3/s. the ratio of runoff to rainfall for this event is 0.44 versus the same value for observation one.

In this part, the results of the model for the DEM with 50 m grid size are presented. The accumulative rainfall graphs are presented in the Fig. 4.8. As it is shown in Figures 4.9 to 4.14, the results of the simulations are in good agreement with the hydrograph measurements.

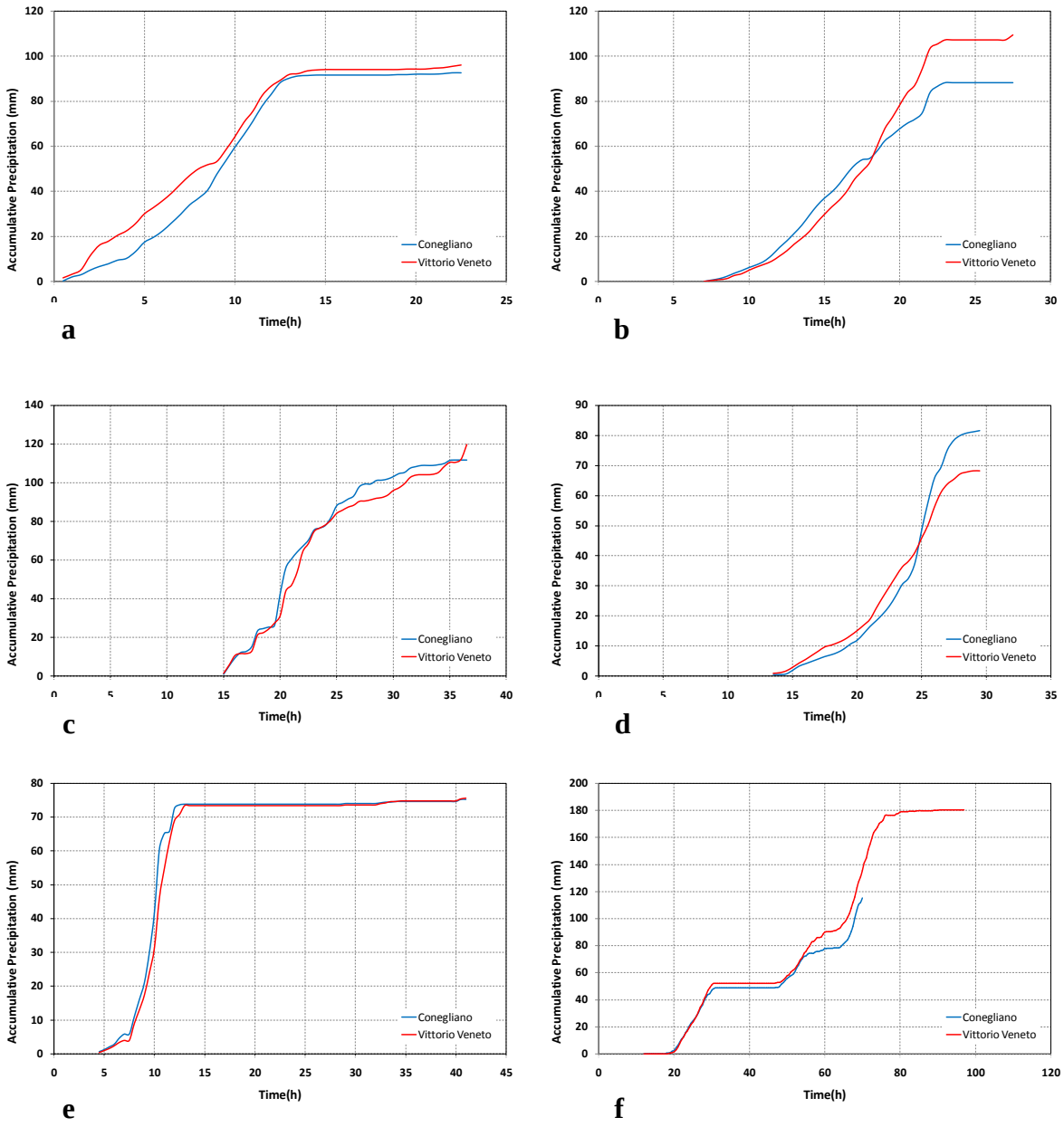

Figure 4.8. Accumulative precipitation measured in stations of Conegliano (blue) and Vittorio Veneto (red) for events a) 20-21 December 1997, b) 6-7 November 2000, c) 10-12 August 2002, d) 21-23 January e) 2003, 31 October-1November 2004 and f) 22-26 December 2009.

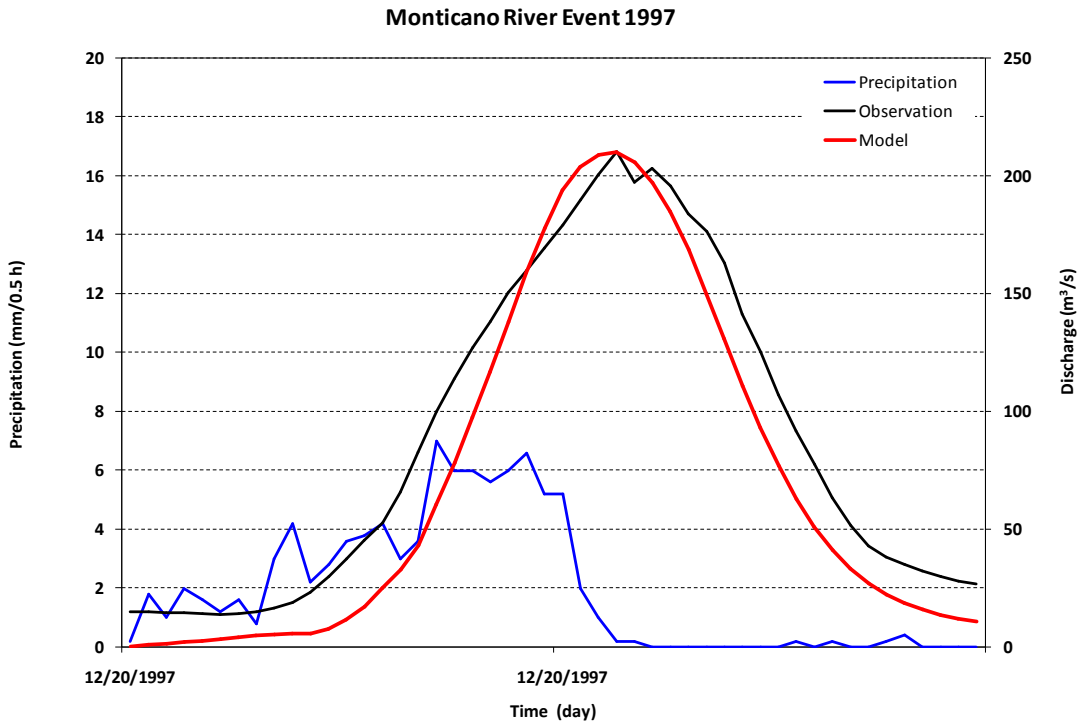

Figure 4.9. Simulation of event December 1997, Monticano River basin. The blue line is precipitation in mm per 30 minutes, black and red lines are hydrograph measurement and model result in m^3/s.

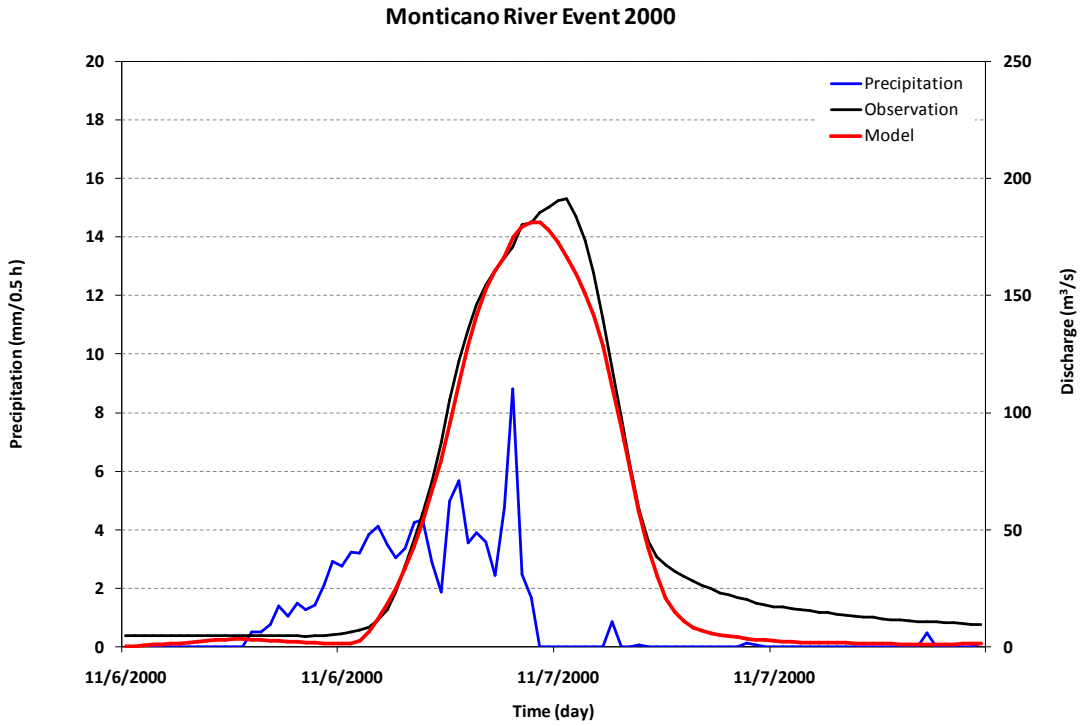

Figure 4.10. Simulation of event November 2000, Monticano River basin. The blue line is precipitation in mm per 30 minutes, black and red lines are hydrograph measurement and model result in m^3/s.

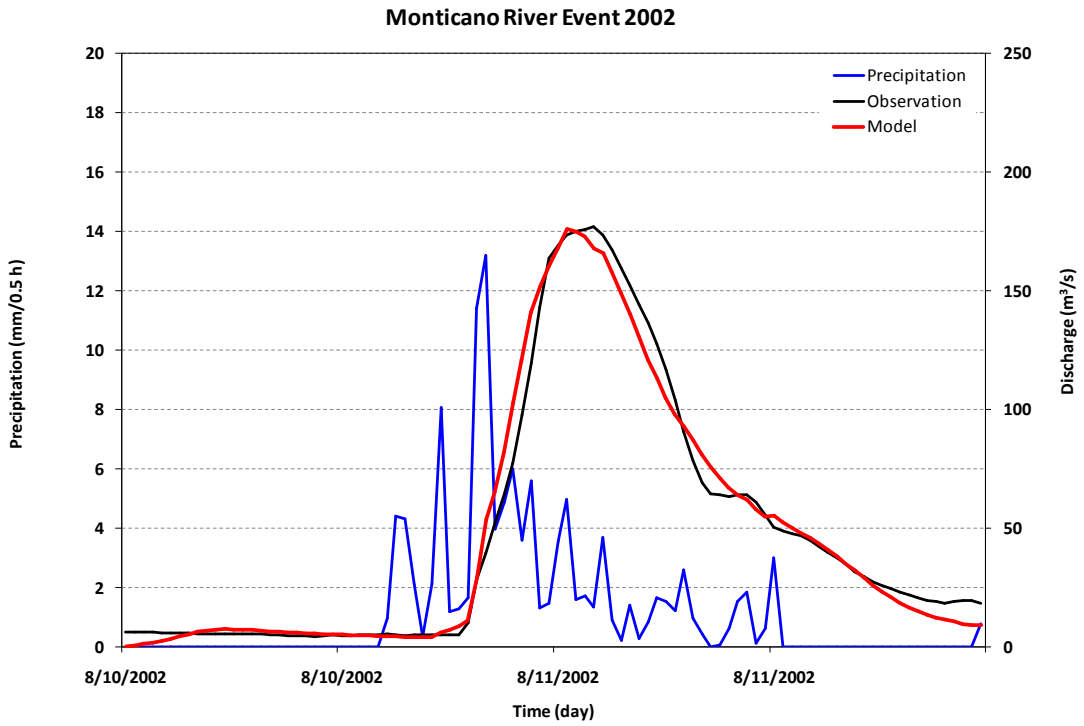

Figure 4.11. Simulation of event August 2002, Monticano River basin. The blue line is precipitation in mm per 30 minutes, black and red lines are hydrograph measurement and model result in m^3/s.

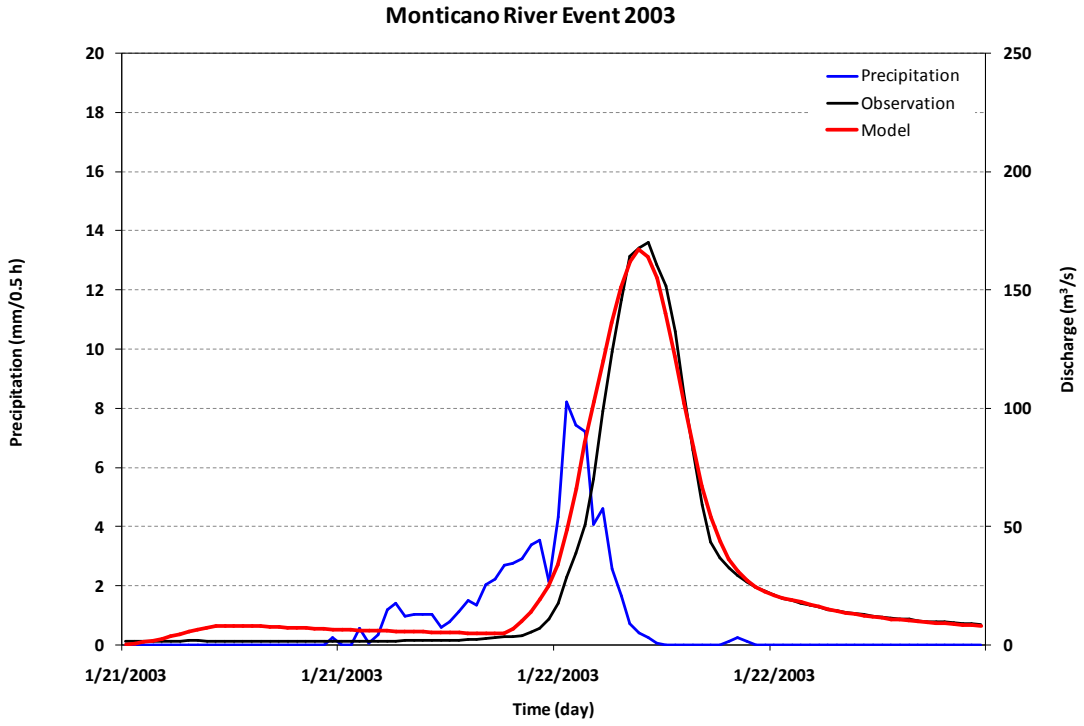

Figure 4.12. Simulation of event January 2003, Monticano River basin. The blue line is precipitation in mm per 30 minutes, black and red lines are hydrograph measurement and model result in m^3/s.

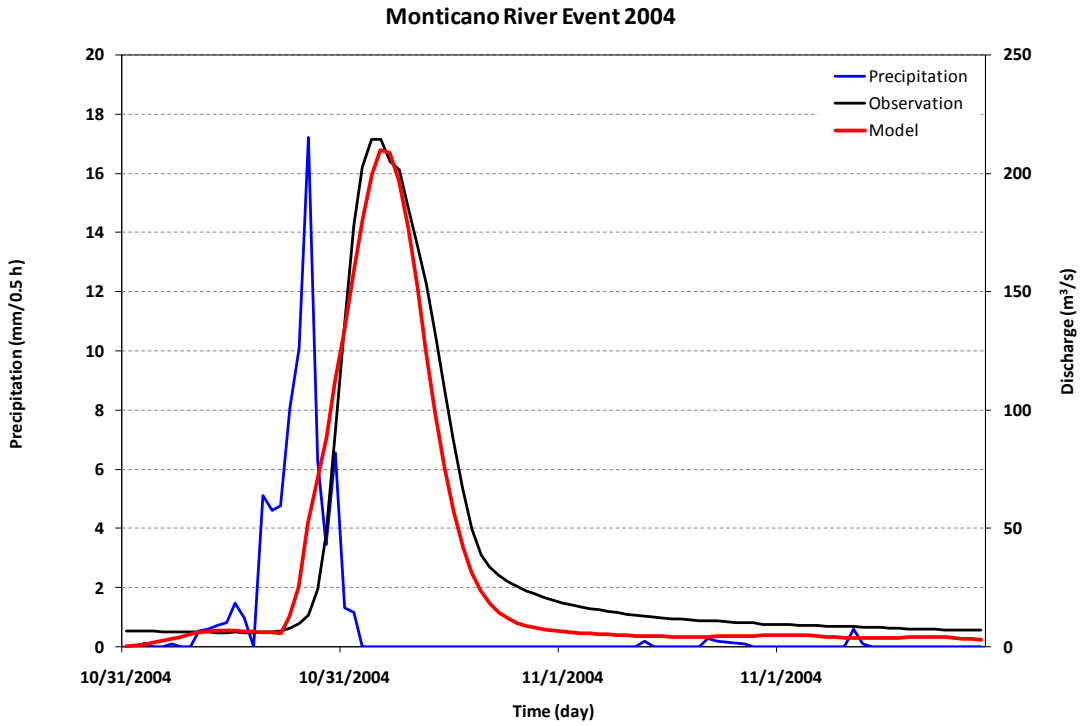

Figure 4.13. Simulation of event October-November 2004, Monticano River basin. The blue line is precipitation in mm per 30 minutes, black and red lines are hydrograph measurement and model result in m^3/s.

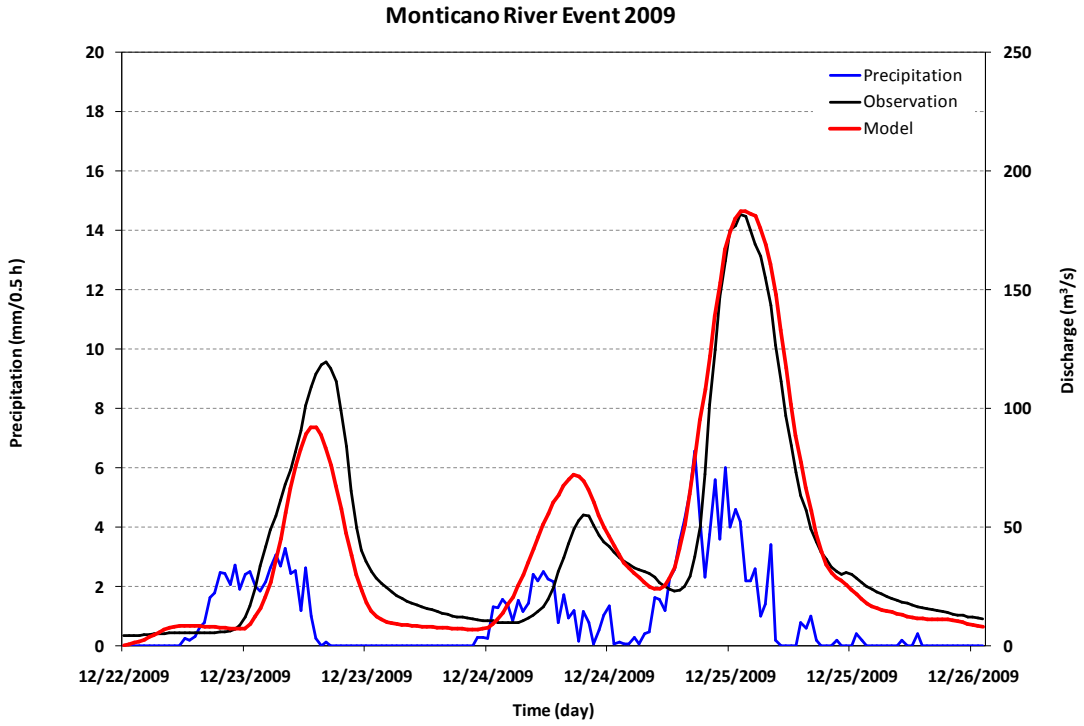

Figure 4.14. Simulation of event December 2009, Monticano River basin. The blue line is precipitation in mm per 30 minutes, black and red lines are hydrograph measurement and model result in m^3/s.

The regression between the observations and simulations are examined. Figure 4.15 show that the simulations fit the observations in a significant way.

The hydrological characteristics of the basin for observed values of all events are presented in table 4.5. The rainfall volume (m^3), base discharge (m^3/s), maximum discharge (m^3/s) and runoff volume (m^3) for each event is calculated. The runoff percentage shows the saturation exceed surface flow and sub-surface flow quantities. The corresponding value of φ has a range of 31 to 46 percent.

Table 4.5. hydrological characteristics of the observed flood events

Date	Duration (h)	Rainfall (m^3)	Q_0 (m^3/s)	Q_{max} (m^3/s)	Runoff (m^3)	φ
20-21 Dec. 1997	24	15742000	345	210.3	7012025	0.45
6-7 Nov. 2000	48	16566500	189	191.3	7694117	0.46
10-12 Aug. 2002	48	19653870	247	177.2	7760871	0.39
21-23 Jan. 2003	48	13107000	187	170	4010125	0.31
31 Oct.-1Nov. 2004	48	12846900	255	214.2	5539430	0.43
22-26 Dec. 2009	85	28597400	139	181.6	12495757	0.44

Similarly, the hydrological characteristics of the basin for simulated values of all events are calculated (Table 4.6). The rainfall volume (m^3) and base discharge (m^3/s) are the same of observational. The maximum discharge (m^3/s) and runoff volume (m^3) derived from simulations are presented to compare with observational quantities. The maximum discharges from modeling show a good agreement with the observed values. The runoff volumes show the same trend with differences for years 1997 and 2000 (Fig. 4.16). The runoff percentage show smaller values comparing the observational values except for 2003, with a range of 36 to 44 percent.

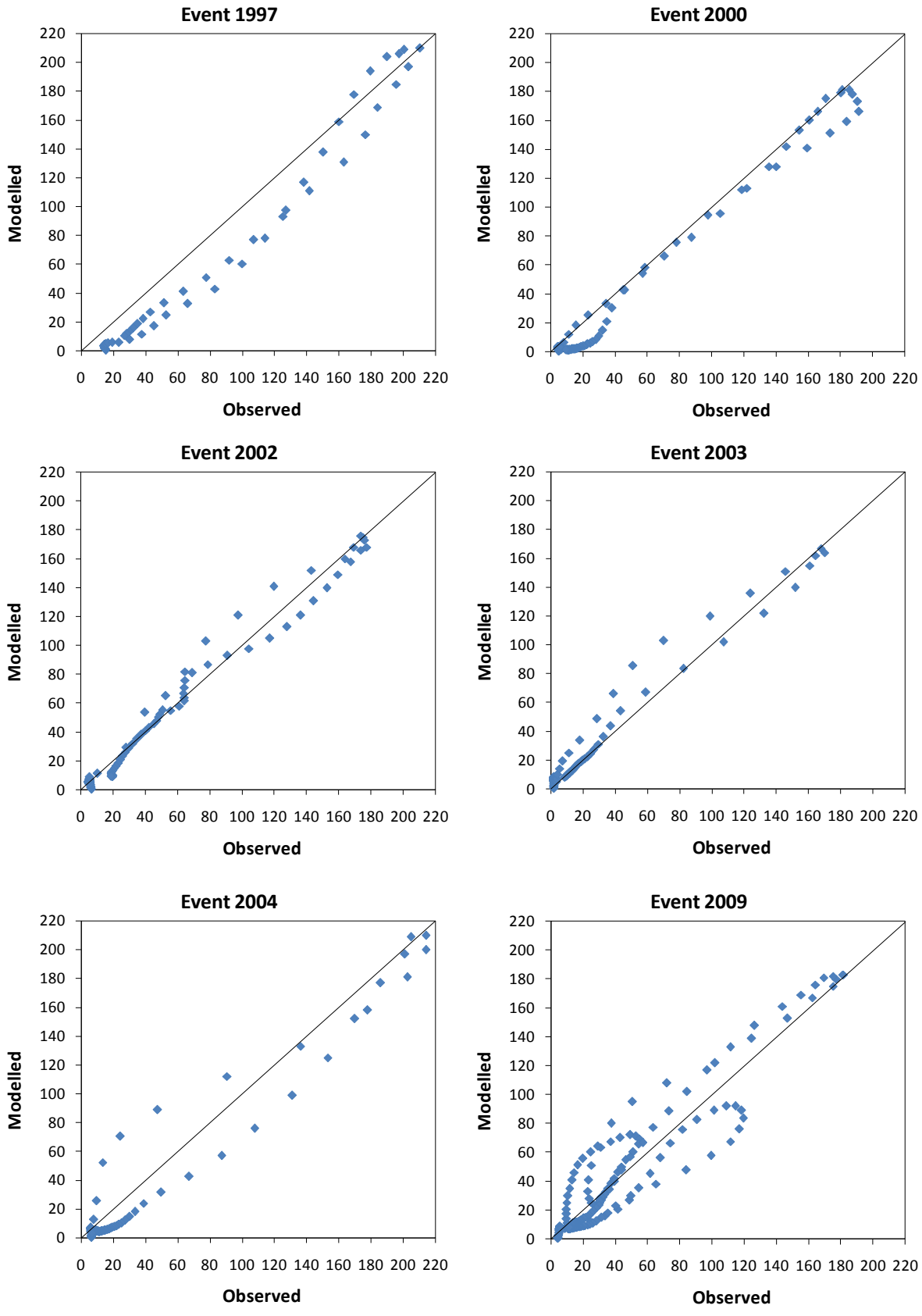

Figure 4.15. Plots comparing modeled and observed discharges for all events.

Table 4.6. hydrological characteristics of the estimated flood events

Date	Duration (h)	Rainfall (m^3)	Q_0 (m^3/s)	Q_{max} (m^3/s)	Runoff (m^3)	φ
20-21 Dec. 1997	24	15742000	345	203	5622080	0.36
6-7 Nov. 2000	48	16566500	189	182	6318022	0.38
10-12 Aug. 2002	48	19653870	247	188	7722889	0.39
21-23 Jan. 2003	48	13107000	187	161	4663786	0.36
31 Oct.-1Nov. 2004	48	12846900	255	191	4615684	0.36
22-26 Dec. 2009	85	28597400	139	180	12537925	0.44

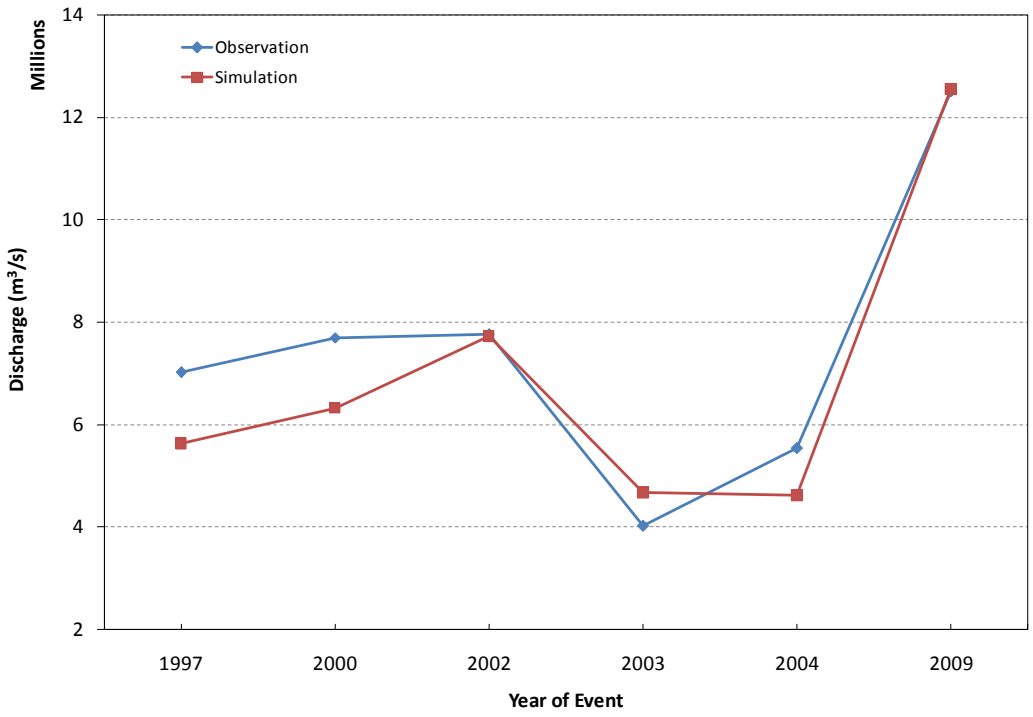

Figure 4.16. Comparing runoff volumes of observation (blue line) and simulation (red line).

As discussed in chapter one, the re-sampled DEM from a high quality data source has still more detail information with respect to the traditional DEM (Vaze and Teng 2007), so we tried to test the effect of some re-sampled DEM from LiDAR data with 25 m (half of the original DEM), 100 m and even a 200 m grid size. To minimize the data volume and computation time and cost (especially in large basins) the best DEM resolution is the largest one with the best fit.

To examine the effect of DEM resolution on the model results, the simulations for all events are performed with the topographic index distribution of above mentioned DEMs. The results (figures 4.17 to 4.22) show that the best fit is of the DEM with 50 m grid size. However, the differences between the other results and observation except of event 2002 are not very large. This is due to this fact that the DEM with 100 m or even 200 m grid size still have enough detail to perform a rough estimation. In other words, this means that the model is sensitive to topographic index distribution but in this basin, which is a small basin the topographic index of different grid sizes, dos not influence very much the model results.

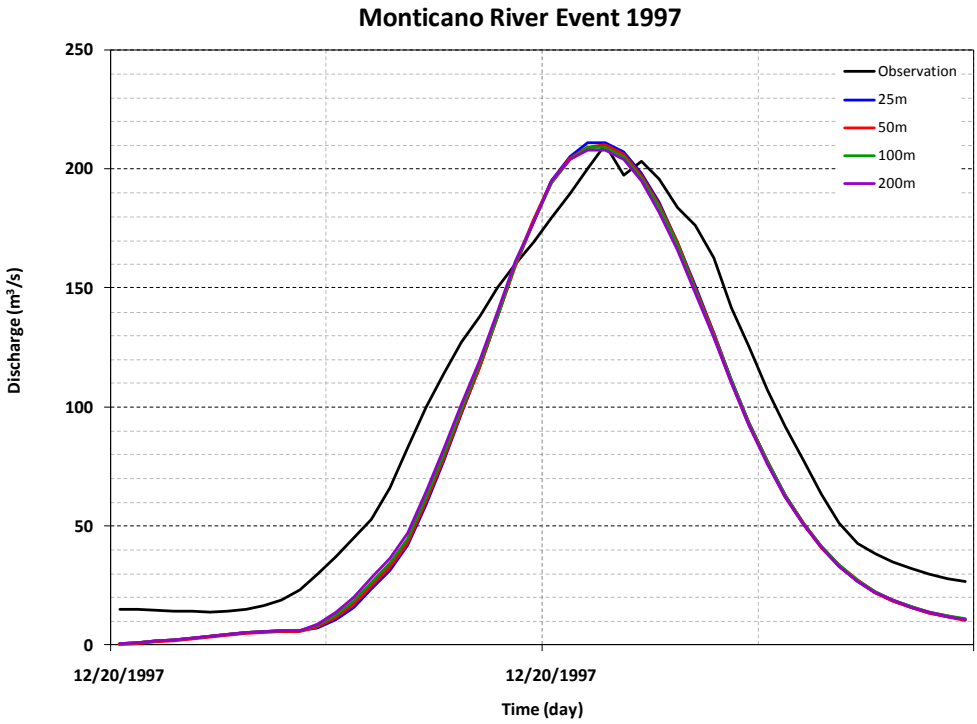

Figure 4.17. Comparing the simulation results Monticano River basin (December 1997). The black line is hydrograph measurement and blue, red, green and violet lines are model result for DEMs with 25m, 50m, 100m and 200m grid size respectively. Units are in m^3/s.

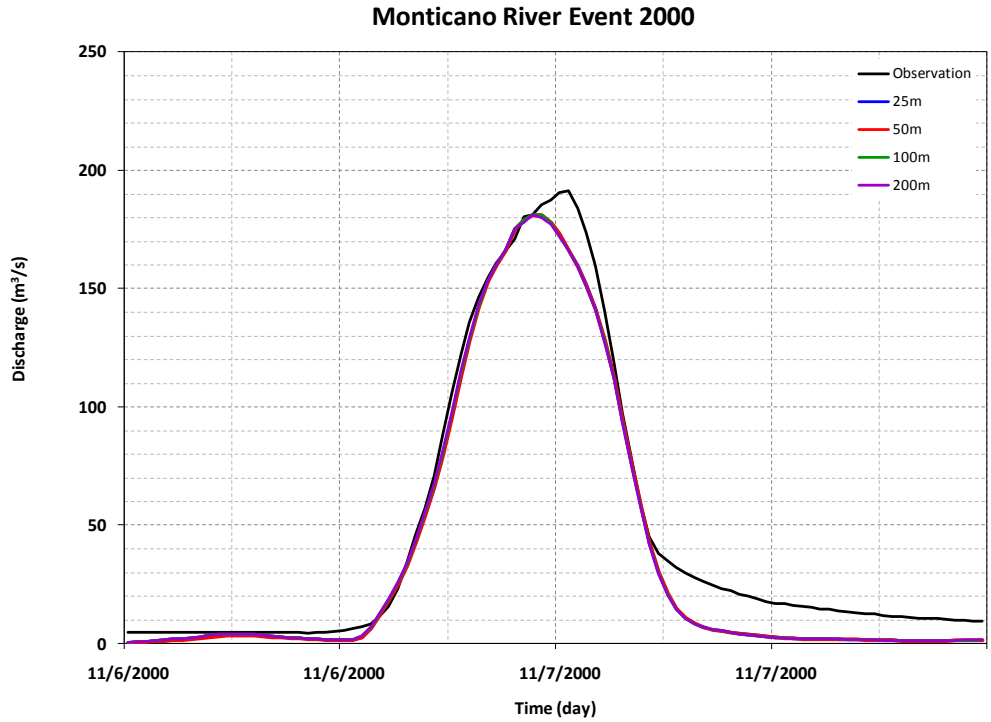

Figure 4.18. Comparing the simulation results Monticano River basin (November 2000). The black line is hydrograph measurement and blue, red, green and violet lines are model result for DEMs with 25m, 50m, 100m and 200m grid size respectively. Units are in m^3/s.

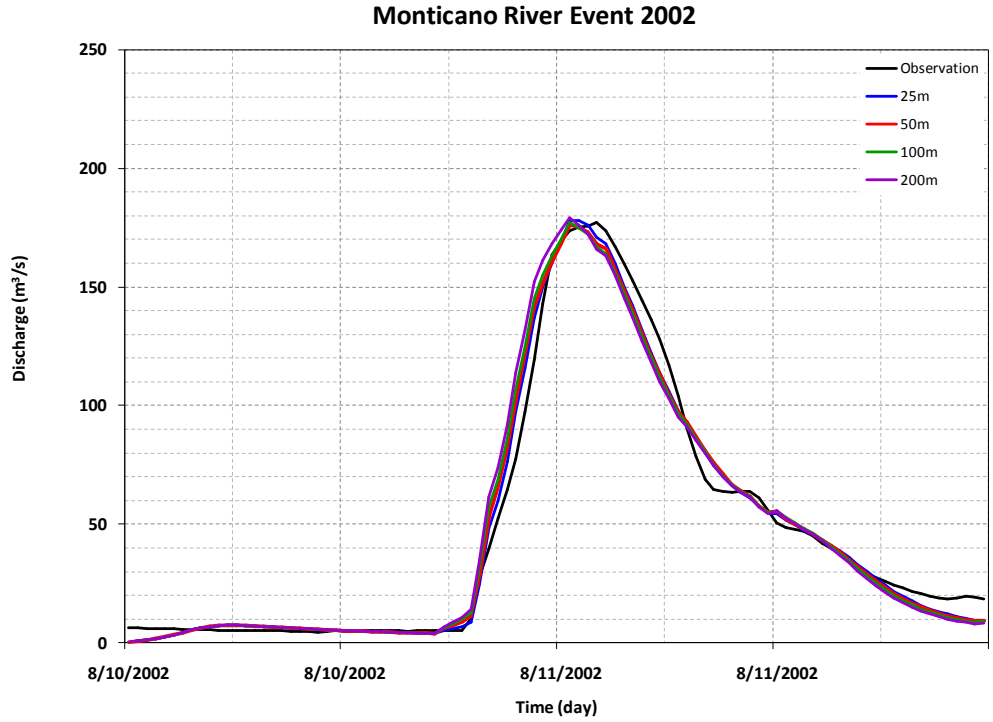

Figure 4.19. Comparing the simulation results Monticano River basin (August 2002). The black line is hydrograph measurement and blue, red, green and violet lines are model result for DEMs with 25m, 50m, 100m and 200m grid size respectively. Units are in m^3/s.

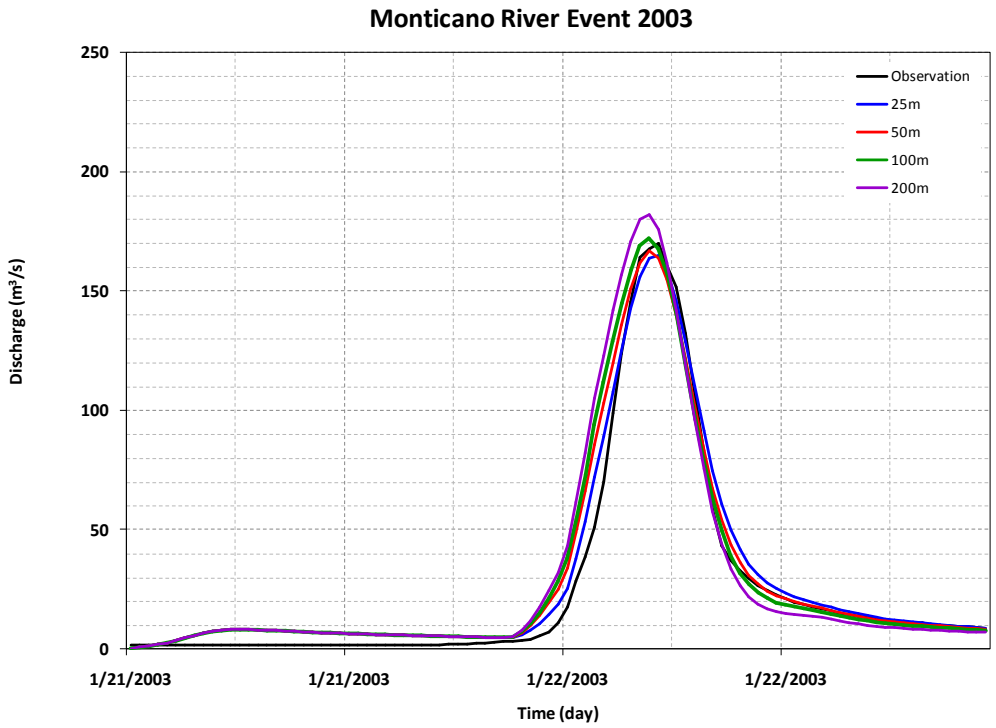

Figure 4.20. Comparing the simulation results Monticano River basin (January 2003). The black line is hydrograph measurement and blue, red, green and violet lines are model result for DEMs with 25m, 50m, 100m and 200m grid size respectively. Units are in m^3/s.

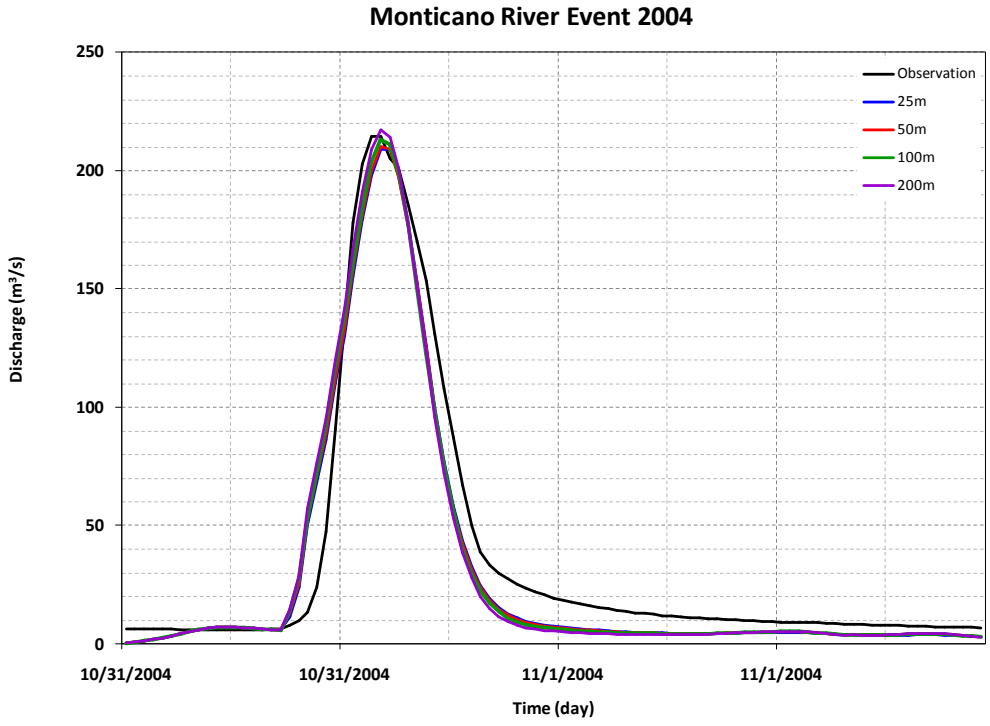

Figure 4.21. Comparing the simulation results Monticano River basin (October-November 2004). The black line is hydrograph measurement and blue, red, green and violet lines are model result for DEMs with 25m, 50m, 100m and 200m grid size respectively. Units are in m^3/s.

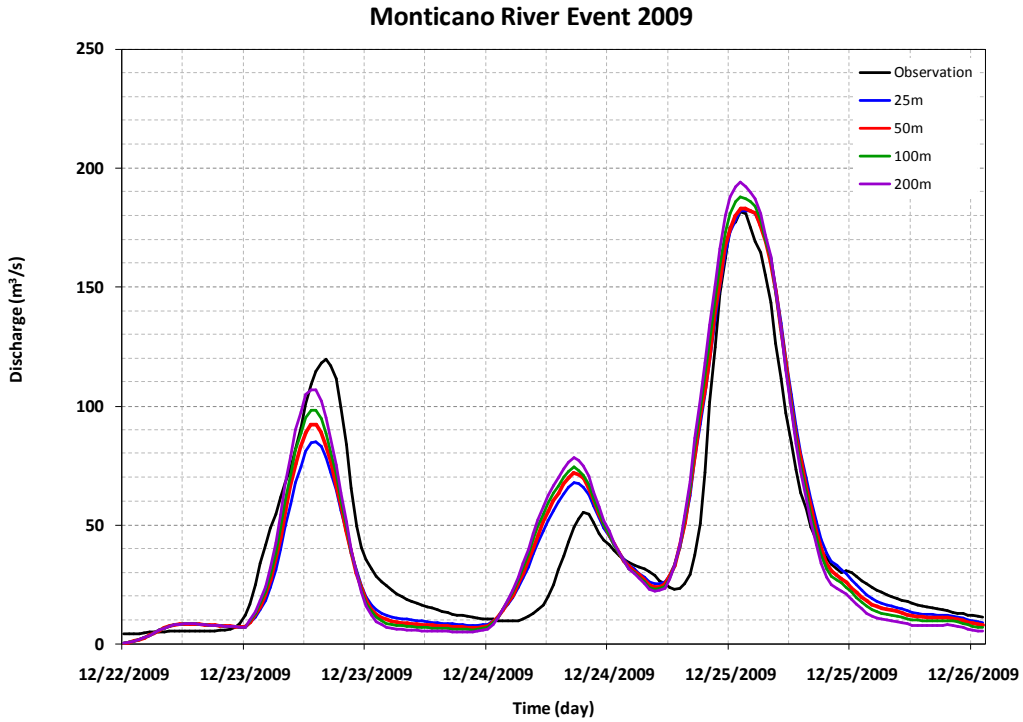

Figure 4.22. Comparing the simulation results Monticano River basin (December 2009). The black line is hydrograph measurement and blue, red, green and violet lines are model result for DEMs with 25m, 50m, 100m and 200m grid size respectively. Units are in m^3/s.

Chapter Five

Discussions and Conclusions

This research approaches semi-distributed rainfall-runoff modeling as an opportunity to understanding of natural systems and addresses questions relevant to predicting streamflow. Chapter 4 presents the main results of this dissertation. Catchment response to rainfall and flood prediction is a crucial hydrological subject that is important for developing policies for more efficient water resources management, flood forecasting, and land use management. Advanced methods in hydrology can help us to understand how we can use the available hydrologic information to predict an unbiased streamflow.

The rainfall runoff models are widely used to simulate the hydrologic processes and predict the catchment response to rain events. The hydrological models can be categorized into lumped models, semi-distributed models and distributed models. TOPMODEL as a semi-distributed model is used to simulate the Monticano River basin.

This dissertation focuses on two main topics related to semi-distributed hydrologic modeling. The first one is applying a semi-distributed model, TOPMODEL, with precipitation observations to show the potential for semi-distributed models to be useful operationally. The second topic is about using high-resolution LiDAR data as topographic data to generate DEM, extracting hydrological features, and investigating the effect of this accurate data on the model result.

Topographic index has an essential role in TOPMODEL, which influences highly the model result, so implementation of very high-resolution LiDAR data will improve the model results.

Accuracy and resolution of DEM from different sources may affect accuracy of hydrological features and parameters extracted from DEM. Therefore, the results of the hydrologic models, which use those parameters as input, may be influenced (Zhang and Montgomery 1994; Saulnier et al., 1997; Su and Bork 2006; Zhao et al., 2010). In addition, the resolution of the topographic data is more significant factor than the methodology used for extracting hydrological features (Barber and Shortridge, 2005).

As discussed in chapter one, using the LiDAR data to generate DEM and extracting hydrological features and topographic index, has numerous advantages with respect to conventional DEMs. Therefore, the LiDAR data with 1-2 points per meter square resolution is used to generate DEM of the study area. In the first step, a continuous terrain model is created using bare ground data. To have a qualitative DEM of the terrain surface by manual editing, the artificial obstacles are removed.

The suggested DEM resolution for TOPMODEL is 50m. To investigate the effect of DEM resolution on the hydrological features, topographic index and finally the model results, DEMs with 25m, 50m, 100m and 200m grid size are generated using ArcGIS 10 (Esri 2010).

Moving from high resolution (25m) to lower resolutions (50m, 100m and 200m), we lose some details of the topography. As shown in table 4.1 the minimum elevation is increased more than one meter, while, the maximum elevation decreased about 69 meters, from 587.95m to 518.48m. The mean and standard deviations indicate that the DEM with 200m grid size is smoother and less variant with respect to DEM with 25m resolution. This means that with higher resolution, more detail of topographic features and slope variations are available and vice versa. Furthermore, as reported by Liu et al. (2005) from higher resolution DEM we can extract the hydrological features with higher accuracy of (Fig. 4.1) which can improve the hydrological model results.

Topographic index (considering T_0, wetness index) is an effective parameter in hydrological modeling that plays a crucial role in TOPMODEL. Spatial distribution of topographic index is a function of DEM resolution and slope. It can be considered as an indicator of the pattern of wetting and drying of the basin. As shown in Fig. 4.2, the area that saturate first, such as valleys, show higher values of topographic index and slopes

show lower values (Beven 1997). Moving from high spatial resolution to lower resolutions, we lose some details especially finer drainage network. As shown in Fig 4.2, in the flat area of the basin, the network detail is almost filtered and this area has close topographic index values.

Comparing the density function of topographic index corresponding to each DEM resolution, indicate that by decreasing the resolution there is a shift toward the higher values (Fig. 4.3) and the topographic constant λ as an indication of whole basin topographic index changes from 7.36 for 25m resolution to 10.32 corresponding to 200 m grid size. Furthermore, there is a distinct difference between the PDF shapes of 25-50 m and 100-200 m resolutions.

Spatial distribution of topographic index can be considered as a map of network of the basin. Of the four different topographic index spatial distribution, the one corresponding to 50m grid size showes very close characteristics to real drainage network derived from LiDAR DEM and provided by ARPAV (Fig. 3.16).

This should be kept in mind that these features are derived from LiDAR data, so even with lower resolutions they include yet enough accurate information with respect to those derived from conventional DEMs.

Finally, we conclude that LiDAR DEMs show great potential to improve hydrologic information for hydrological modeling purposes. The stream network modeled using the LiDAR DEM is the most accurate representation of the actual network comparing the other conventional methods. This improvement over conventional DEMs is mainly due to the increased point density, resolution and accuracy of LiDAR DEMs. Altering the LiDAR DEM appropriately allows modeling of the impact of manufactured features, such as road networks, on hydrology (Murphy et al., 2008).

Application of the TOPMODEL model to the Monticano River basin until its outlet in Fontanelle Station reveals that the model successfully simulates flood levels, with respect to both their extent and to peak time. The simulation is performed for six selected events: 20-21 December 1997, 6-7 November 2000, 10-12 August 2002, 21-23 January 2003, 31 October-1November 2004 and 22-26 December 2009.

The sensitivity analysis is performed for two parameters; scale parameter m and lateral transmissivity T_0. From these results, we note that the coefficient m affects much more than T_0 on the hydrograph shape and peak value of the flood wave (Figures 4.6 and 4.7). This is because m represents the rate of decay of the permeability in the unsaturated soil increases

the deficit of saturation, which determines the inflow to the phase, saturated. In addition, it also governs the dynamics of expansion and contraction of the contributing areas in response to rain.

High values of *m* considerably increase the capacity of infiltration of the ground, while low values generate a shallow depth infiltration, thus the model in a saturated zone in a shorter time, generates a greater surface runoff. Therefore, in a physically based model, *m* is the parameter that controls the thickness of soil that is actually affected by the phenomena of infiltration and water storage.

The simulation is performed for different events with calibrated parameters. The peak values, shape of observed the hydrograph and timing of the events are well predicted. However, regarding event 2000 the peak value shows lower estimation. Comparing the simulated values versus observations (Fig. 4.15) reveal, the model outcomes are quite respectable. The event 1997 and 2004 show somewhat underestimation and event 2003 is slightly overestimated. The event 2009 which is a bit complex, but is in good agreement with observations.

The estimation of runoff volumes of each event and comparing to observations reveal quite good agreement (Fig 4.16).

The runoff to rainfall ratio for the simulated runoff values shows a range of 0.36 to 0.44. These values are lower with respect to those of observations, which mean that simulated values are underestimated (table 4.4 and 4.5). This can be due to the skewness of the predicted discharges that are slightly underestimated (Figures 4.9 to 4.14).

To determine the effect of DEM resolution on the model results, the topographic index distribution for different grid sizes are considered as input for TOPMODEL. Obviously, the results are different, but the differences are very small except for events 2003 and 2009. The results of simulations based on 25m grid size are very close to those of 50m grid size, while the simulated discharges using 100m and 200m grid size are overestimated.

The efficiency of the simulations show relatively high values for all events. It is calculated for all simulated events using different topographic index distributions (Table 4.4). The corresponding efficiency of simulation based on DEM with 25m resolution show slightly higher values. This means that in spite of suggested 50m grid size as optimum resolution for TOPMODEL, in this study, which uses LiDAR data, a higher resolution (25m) which is more accurate (for extracting hydrological features and topographic index),

have a better output. As it is evident the efficiency decreases with increasing the grid size (Table 4.4).

The high efficiency values of simulations for the six events of Monticano River basin suggest that applying a semi-distributed model, which is less complicated from point of view of application and parameterization and calibration, with high quality observations of topographic data and hydrological data can provide sufficiently satisfying results. This is a point for water resource management especially flood prediction for the intensive rainfall events.

Bibliography

- Agenzia Regionale per la Prevenzione e Protezione Ambientale (ARPA) del Veneto, 2009. Valutazione della permeabilità e del gruppo idrologico dei suoli del veneto, 19 pp.

- Agenzia Regionale per la Prevenzione e Protezione Ambientale (ARPA) del Veneto, 2010. Livelli e portate medie giornaliere del fiume Monticano a Fontanelle negli anni 2004-09, 24 pp.

- Agenzia Regionale per la Prevenzione e Protezione Ambientale (ARPA) del Veneto, 2010b. Ricostruzione dei profili di velocità per la restituzione di misure correntometriche condotte in condizioni di piena, 22 pp.

- Anderson, M.G. and Burt, T. P., 1985. Modelling strategies. In: Hydrological Forecasting, M. G. Anderson and T. P. Burt, John Wiley & Sons Ltd.: pp. 1-13.

- Barber, C. P. and Shortrudge, A. M., 2004. Light Detection and Ranging (LiDAR) – Derived Elevation Data for Surface Hydrology Applications, Institute of Water Research, Michigan State University.

- Barber C.P., and Shortridge A.M.,, 2005. Terrain representation, scale, and hydrologic modeling: does LiDAR make a difference? Autocarto 2005. Las Vegas, Nevada, March 21-23.

- Beven, K. J. 1986a. `Runoff production and flood frequency in catchments of order n: an alternative approach', in Gupta, V. K., Rodriguez-Iturbe, I., and Wood, E. F. (Eds), Scale Problems in Hydrology, Reidel, Dordrecht, pp. 107-131.

- Beven, K. J., 1986b. Hillslope runoff processes and flood frequency characteristics in Hillslope processes, edited b y A.D. Abrahams, pp. 187- 202, Allen and Unwin, Winchester, Mass.

- Beven, K. J. and Wood, E. F. 1983. Catchment geomorphology and the dynamics of runoff contributing areas, J. Hydrol., 65, 139-158.

- Beven K.J., Lamb R., Quinn P., Romanowicz R., e Freer J. 1995. 'TOPMODEL', in Singh, V.P. (Ed), Computer Models of Watershed Hydrology. Water Resource Publications, Colorado. pp. 627 – 668.

- Beven, K. J. (1997) TOPMODEL: A critique, Hydrol. Processes. 11, 1069-1085.

- Beven, K.J., 2001. Rainfall-Runoff Modeling, The Primer. John Wiley and Sons, Chichester, 360 p.

- Beven, K. J. and Kirkby, M. J. 1979, A physically based, variable contributing area model of basin hydrology. Hydrol. Sci. Bull., 24, 43–69.

- Boggs, G.S., Evans, K.G., and Devonport, C.C., 2001. ArcEvolve: A Suite of GIS Tools for Assessing Landform Evolution. Proceedings of the 6th International Conference on GeoComputation, University of Queensland, Brisbane, Australia, 24 - 26 September 2001.

- Boyle, D.P., Gupta, H.V., Sorooshian S., Koren V., Zhang Z., and Smith M. 2001: Towards improved streamflow forecasts: The value of semi-distributed modeling. Water Resources Research, AGU, 37(11), 2749-2759.

- Corradini, C., Morbidelli, R., Saltalippi, C., Melone, F.2002: An adaptive model for flood forecasting on medium size basins. Proceedings of the IASTED International Conference "Applied Simulation and Modelling", Crete, Greece, June 25-28 2002, pp. 555-559.

- Cunderlik J.M., 2003. Hydrologic Model Selection for the CFCAS. Project: Assessment of Water Resources Risk and Vulnerability to Changing Climate Conditions. Project Report I.: pp. 1-38. Danish Hydraulic Institute (DHI), 1998. MIKE SHE - User Guide and Technical Reference Manual.

- Esri 2011. Lidar Analysis in ArcGIS 10 for Forestry Applications, an Esri white paper, 53 pp.

- Garbrecht, J. and Martz, L. W. (1999), Digital Elevation Model Issues In Water Resources Modeling, 19th ESRI International User Conference, Environmental Systems Research Institute.

- Gomez A., Serrano J., Casalprim D., 2005, Generation of a DTM based on LiDAR data for the definition of hydraulic models. XXII Int. Cartographic Conference (ICC2005), A Coruña, Spain, 11-16 July 2005 (CD).

- Gross, S. B. (2003), LIDAR (Light Detection and Ranging), Accessed: 06 May 2005, http://www.sbgmaps.com/lidar.html

- Hodgson, M. E., Jensen, J., Raber, G., Tullis, J., Davis, B. A., Thompson, G. and Schuckman, K., 2005. An Elevation of LiDAR-Derived Elevation and Terrain Slope in Leaf-off Conditions, Photogrammetric Engineering and Remote Sensing, 71(7): 817-823.

- Kenward, T., Lettenmaier, D. P., Wood, E. F. and Fielding, E. (2000), Effects of Digital Elevation Model Accuracy on Hydrologic Predictions, Remote Sensing of Environment, 74(3): 432-444.

- Kirkby, M. J. 1975. `Hydrograph modelling strategies', in Peel, R., Chisholm, M., and Haggett, P. (Eds), Process in Physical and Human Geography, Heinemann, London. pp. 69-90.

- Kirkby, M. J. and Weyman, D. R. 1974. `Measurements of contributing area in very small drainage basins', Seminar Series B, No. 3. Department of Geography, University of Bristol, Bristol.

- Lastoria, B., 2008: Hydrological processes on the land surface: A survey of modeling approaches. FORALPS Technical Report, 9. Università degli Studi di Trento, Dipartimento di Ingegneria Civile e Ambientale, Trento, Italy, 56 pp.

- Liu, X., Peterson, J., and Zhang, Z., 2005. High-resolution DEM generated from LiDAR data for water resource management, in Proceedings of International Congress on Modelling and Simulation 'MODSIM05', 12 - 15 December 2005, Melbourne, Australia, 1402-1408.

- Lohr, U., 1998. Digital Elevation Models by Laser Scanning, Photogrmmetric Record, 16(91): 105-109.

- Maidment, D.R., 1996. GIS and Hydrologic Modeling. An Assessment of Progress, Presented at the Third International Conference on GIS and Environmental Modeling, Santa Fe, New Mexico, 22-26.

- Melone F., Barbetta S., Diomede T., Peruccacci S., Rossi M., Tessarolo A., 2005. Review and selection of hydrological models – Integration of hydrological models and meteorological inputs. RISK AWARE - INTEREG IIIB CADSES programme.

- Narula K.K., Bansal N.K. and Gosain A.K., 2002. Hydrological sciences and recent advances: a review. TERI Information Digest on Energy and Environment: Vol. 1, Num. 1, pp. 71-93.

- Nash J. E. and Stucliffe J. V. 1970. River flow forecasting through conceptual models 1. A discussion of principles. J. of Hydrology 10, 282-290.

- Perrin C., Andréassian V. and Michel C., 2002. State-of-the-art for Precipitation-runoff Modelling. In: State-of-the-Art Report on Quality Assurance in modelling related to river basin management, HarmoniQuA-report, D-WP1-1: 5, pp.1-10.

- Quinn, P. F., Beven, K. J., and Lamb, R. 1995. `The ln(a/tanβ) index: how to calculate it and how to use it in the TOPMODEL framework', Hydrol. Process., 9, 161-182.

- Saulnier, G.-M. 1996. `Information pedologique spatialiseÂe et traitements topographiques ameÂ lioreÂ s dans la modeÂ lisation hydrologique par TOPMODEL', PhD Thesis, Institut National Polytechnique de Grenoble, Grenoble, France.

- Saulnier G-M, Obled C, Beven KJ. 1997. Analytical compensation between DTM grid resolution and effective values of saturated hydraulic conductivity within the TOPMODEL framework. In Distributed Hydrological Modelling: Applications of the TOPMODEL concept, Beven KJ (ed.). Wiley: Chichester; 249–264.

- Singh V.P., 1995. Computer Models of Watershed Hydrology. Water Resources Publications, Highlands Ranch, Colorado.

- Su, J. and E. Bork, 2006. Influence of vegetation, slope, and LiDAR sampling angle on DEM accuracy. Photogrammetric Engineering & Remote Sensing, 72(11), pp. 1265-1274.

- Todini, E.: The ARNO rainfall-runoff model. Journal of Hydrology, 175(1-4), 339-382, 1996.

- Vaze J. and Teng J., 2007. Impact of DEM Resolution on Topographic Indices and Hydrological Modelling Results. MODSIM 2007 International Congress on Modelling and Simulation. Modelling and Simulation Society of Australia and New Zealand, December 2007.

- World Meteorological Oganization, Simulated Real Time Intercomparison of Hydrological Models, Operational Hydrology Report No. 38, Geneva, 1992.

- Zhang W, Montgomery DR. 1994. Digital elevation model grid size, landscape representation and hydrologic simulations. Water Resources Research 30: 1019–1028.

- Zhao Z., Benoy G., Chow T.L., Rees H.W., Daigle J.L. and Meng F.R, 2010. Impacts of accuracy and resolution of conventional and LiDAR based DEMs on parameters used in hydrologic models. Water Resource Manage, 24:1363-13980. DOI 10.1007/s11269-9503-5.